Monazite-(Ce) in Hercynian granites and pegmatites of the Bratislava Massif, Western Carpathians: compositional variations and Th-U-Pb electron-microprobe dating

Pavel Uher[1], Milan Kohút[2], Martin Ondrejka[1], Patrik Konečný[2] & Pavol Siman[3]

[1]Department of Mineralogy and Petrology, Faculty of Natural Sciences, Comenius University in Bratislava, Mlynská dolina G, 842 15 Bratislava, Slovakia; puher@fns.uniba.sk
[2]Dionýz Štúr State Institute of Geology, Mlynská dolina 1, 817 04 Bratislava, Slovakia
[3]Geological Institute, Slovak Academy of Sciences, Dúbravská cesta 9, 840 06 Bratislava, Slovakia

AGEOS

Monazit-(Ce) v hercýnskych granitoch a pegmatitoch bratislavskeho masívu (Západné Karpaty): variácie chemického zloženia a Th-U-Pb datovanie pomocou elektrónovej mikroanalýzy

Abstract: Monazite-(Ce) represents a characteristic magmatic accessory mineral of the Hercynian peraluminous S-type granites to granodiorites and related granitic pegmatites of the Bratislava Granitic Massif (BGM), Malé Karpaty Mountains, Central Western Carpathians, SW Slovakia. Monazite forms euhedral to subhedral crystals, up to 200 μm in size, usually it is unzoned in BSE, rarely it reveals oscillatory or sector zoning. Thorium concentrations of 2 to 9 wt. % ThO_2 (≤ 0.09 apfu) and local elevated uranium contents (≤ 4.3 wt. % UO_2, ≤ 0.04 apfu) are characteristic for the pegmatite monazites. Both huttonite $ThSiREE_{-1}P_{-1}$ and cheralite $Ca(Th,U)REE_{-2}$ substitutions took place in the studied monazite. Electron-microprobe Th-U-Pb monazite dating of the granites and pegmatites gave an isochron age of 353 ± 2 Ma (MSWD = 0.88, n = 290), which confirmed the meso-Hercynian, Lower Carboniferous (Mississipian) magmatic crystallization. An analogous age (359 ± 11 Ma) was obtained from monazite from adjacent paragneiss, corresponding to the age of the Hercynian contact thermal metamorphism related to the granite intrusion of BGM. Monazite in some granite shows also older clastic or authigenic grains or zones (~ 505 to 400 Ma, with maximum of 420 ± 7 Ma) which probably represents inherited material from the Lower Paleozoic metapelitic to metapsammitic protolith of BGM.

Key words: monazite-(Ce), Th-U-Pb EMP dating, Lower Carboniferous, granitic rocks, pegmatites, Bratislava Granitic Massif, Western Carpathians

1. INTRODUCTION

Accessory monazites are essential carriers of REE in common granitic and metamorphic rocks (together with allanite, apatite, xenotime, and zircon), and their detailed study of composition and breakdown processes represent important tools for understanding the petrogenesis and evolution of the parental rock (e.g., Montel, 1993; Bea, 1996; Bingen et al., 1996; Finger et al., 1998; Broska & Siman, 1998; Förster, 1998; Zhu & O`Nions, 1999; Johan & Johan, 2005; Finger & Krenn, 2007; Krenn & Finger, 2007; Petrík & Konečný, 2009; Ondrejka et al., 2007, 2012, among many others). The presence of U, Th, and radiogenic Pb as well the almost total absence of common Pb in monazite enable us to date the mineral's crystallization or alteration by the chemical, electron-microprobe method (e.g., Suzuki et al., 1991; Montel et al., 1996; Scherrer et al., 2000; Cocherie & Albarede, 2001; Williams et al., 2006).

Monazite-(Ce) is a widespread accessory mineral and essential REE-bearing phase in the Bratislava Granitic Massif (BGM), Slovakia. Investigations of accessory minerals revealed a systematic presence of monazite in the BGM (Mišík, 1955; Veselský, 1972; Veselský & Gbelský, 1978) and their affinity to the monazite-series of granitic rocks (Broska & Uher, 1991). Field, K-Ar, and Rb-Sr isotopic data showed mainly Hercynian, Lower Carboniferous ages of the BGM (Koutek & Zoubek, 1936; Cambel & Valach, 1956; Kantor, 1959, 1961; Bagdasaryan et al., 1977, 1982; Cambel et al., 1979, 1990). In addition, preliminary results of the monazite electron-microprobe dating yielded age of 355±18 Ma (Finger et al., 2003) identical to a zircon SHRIMP age of 355±5 Ma for the BGM (Kohút et al., 2009).

Our contribution represents the first systematic study of the chemical composition and electron-microprobe dating based on a large analytical set of monazite-(Ce) analyses from the BGM, a typical example of an orogenic-related, S-type granite-pegmatite suite. The study contributes to our knowledge of the granitic protolith, the origin of monazite as a principal carrier of REE as well as the emplacement of the parental granitic rocks as an integral part of meso-Hercynian subduction to collisional events at the Gondwana frontier.

Manuscript received 10 July 2013
Revised version accepted 9 September 2014

2. REGIONAL GEOLOGY

The granitic rocks forms the dominant part of the Malé Karpaty Mountains pre-Alpine basement between the towns of Bratislava and Modra, SW Slovakia (Fig. 1), as well as in a small territory of the Hundsheim Hills on the opposite side of the Danube river valley near Hainburg town, NE Austria. Two principal Hercynian granitic intrusions were emplaced in the Malé Karpaty Mts.: the Bratislava and Modra massifs.

The fundamental rock types of the BGM are muscovite-biotite monzogranites to granodiorites, less frequently there occur leucocratic two-mica to muscovite syenogranites, biotite leucotonalites, and small bodies of biotite-amphibole diorites (Cambel & Valach, 1956; Cambel & Vilinovič, 1987; Kohút et al., 2009, and references therein). The granitic rocks are usually medium-grained equigranular, rarely porphyric with K-feldspar phenocrysts. Systematic petrographic and geochemical studies of the BGM indicated their orogen-related, peraluminous calc-alkaline character and S-type affinity, whereas the biotite tonalites, granodiorites to granites of the Modra Granitic Massif (MGM) show I-type affinity (Cambel & Vilinovič, 1987; Petrík & Kohút, 1997; Petrík et al., 2001; Broska & Uher, 2001; Kohút et al., 2009).

Dikes of granitic pegmatites and aplites are widespread in the

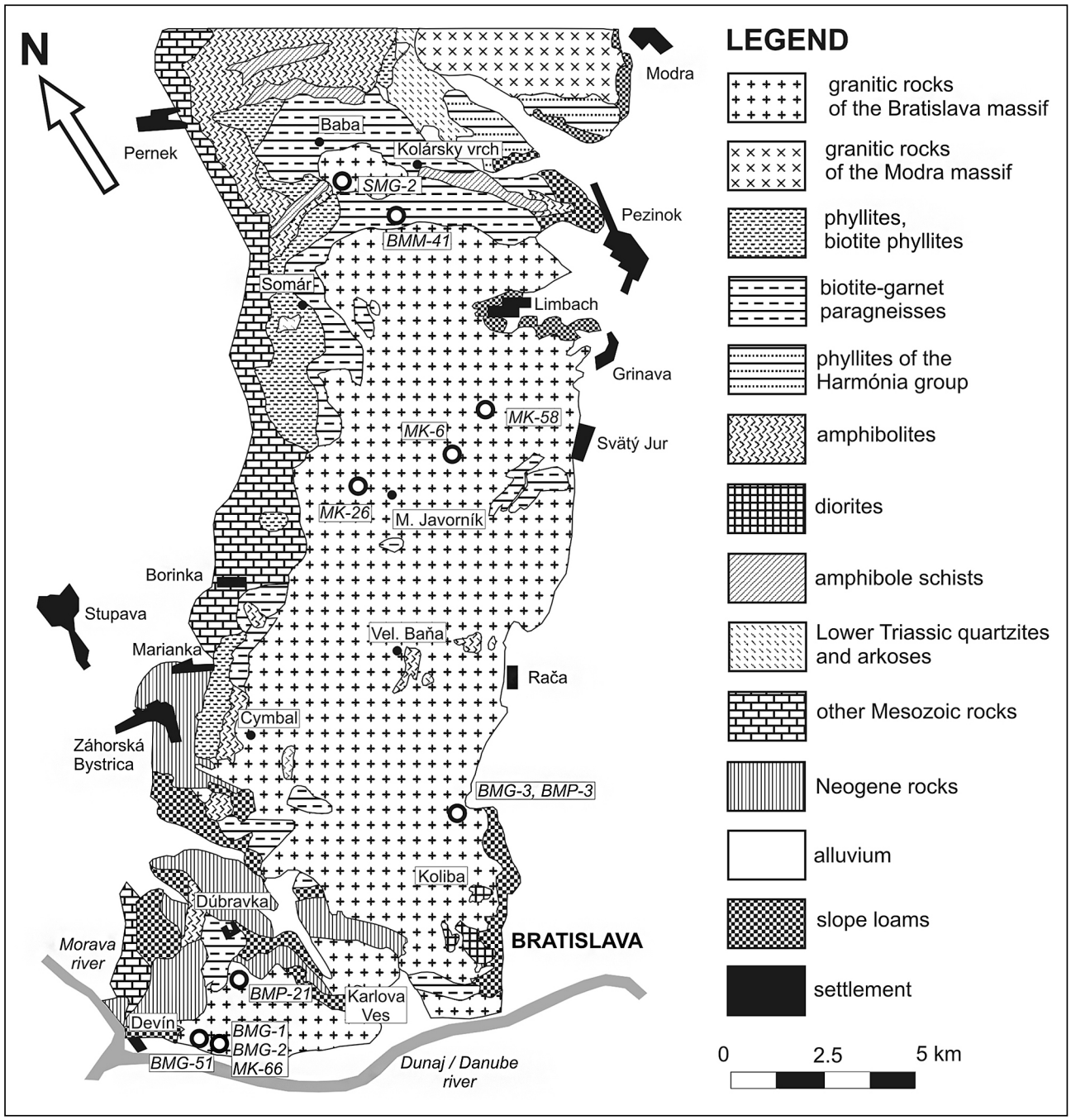

Fig. 1. Simplified geological map of the Bratislava Massif area (adapted according to Cambel & Vilinovič, 1987) with sample location.

BGM but relatively scarce in the MGM (e.g., Koutek & Zoubek, 1936; Cambel & Valach, 1956; Cambel & Vilinovič, 1987). The pegmatite dikes, usually up to 1–2 m thick, commonly show zonal structure with graphic, blocky K-feldspar, coarse-grained alkali feldspar-quartz-muscovite-(biotite) and blocky quartz core zones, locally with late fan-like muscovite and saccharoidal albite-rich replacement zones (Dávidová, 1970). The most fractionated granitic pegmatites of the BGM contain accessory beryl and Nb-Ta oxide minerals (e.g., Uher, 1994; Uher & Broska, 1995; Uher et al., 2010; Chudík et al., 2011) and they could be classified as beryl-columbite subgroup of the rare-element class of granitic pegmatites (sensu Černý & Ercit, 2005).

Published geological and geochronological data show Hercynian (Variscan), early Carboniferous age of the BGM and MGM intrusions and solidification (e.g., Koutek & Zoubek, 1936; Cambel & Valach, 1956; Bagdasaryan et al., 1982; Cambel et al., 1990; Finger et al., 2003; Kohút et al., 2009, see Discussion and conclusion chapter for details). The granitic rocks of the BGM and MGM exhibit distinct intrusive and thermal metamorphic contacts with adjacent metapelites to metapsammites and metabasic rocks of the Pezinok and Pernek Group (Ivan et al., 2001; Putiš et al., 2004; Ivan & Méres, 2006). The pre-metamorphic lithology of the Pezinok Group represents a relatively huge flysch sequence of pelitic and psammitic sediments, mainly rhythmically alternating sandstones and shales, locally with quartzitic, lydite, carbonate, and basaltic tuffaceous horizons, originated mainly on a continental margin (Putiš et al., 2004). Geochemical study of the Pezinok Group revealed a presence of immature greywacke rocks derived from the active continental margin near ensialic island arc with acid to intermediate magmatic rocks and the whole rock sequence represents a remnant of the back-arc rift basin filling (Ivan et al., 2001; Méres, 2005; Ivan & Méres, 2006). On the other hand, the Pernek Group represents an ophiolite sequence of metamorphosed basalts, gabbros, and pelagic pelitic rocks enriched in organic carbon substance with stratiform pyrite-pyrrhotite layers, a remnant of oceanic crust (Ivan et al., 2001; Putiš et al., 2004; Méres, 2005; Ivan & Méres, 2006). Rare microfossil remnants indicate the late Silurian, Devonian to early Carboniferous age of both the Pezinok and Pernek Group (Čorná, 1968; Cambel & Čorná, 1974; Cambel & Planderová, 1985).

The Hercynian contact thermal metamorphism of the Pezinok and Pernek groups due to intrusion of the BGM and MGM attains typical conditions of the amphibolite facies. The metamorphic conditions of the Pezinok Group due to the intrusion of the BGM were estimated at temperature up to 500–580°C and pressure of 3 to 3.5 kbar (Korikovsky et al., 1984; Korikovsky in Krist et al., 1992). However, thermodynamic modelling and geothermobarometric calculations show higher metamorphic conditions: T ~550 to 620°C and P ~5 to 7 kbar for staurolite-sillimatite and staurolite-garnet-bearing metapelites (Cambel et al., 1981; Dyda, 1997, 2000; Vojtko et al., 2011[a,b]). The following metamorphic zones were developed in the metapelites to metapsammites of the contact thermal metamorphic aureole of the Pezinok Group: biotite, garnet, staurolite-chlorite, and staurolite-sillimanite zone (Korikovsky et al., 1984; Korikovsky in Krist et al., 1992).

3. EXPERIMENTAL METHODS

Monazites were analysed using Cameca SX-100 microprobe at the Department of the Electron Microanalysis, State Geological Institute of Dionýz Štúr, Bratislava. Monazite dating requires special measurement conditions since the calculated age strongly depends on the precise measurement of Pb, U, Th, and Y. We are using 15 kV accelerating voltage, 100 nA beam current and variable counting times depending on the measured element, Pb 150 s, Th 45 s, U 75 s, Y 45 s and all other elements 25–35 s. The elements are calibrated using synthetic or natural standards: all 14 REE elements were calibrated from synthetic phosphates, P was calibrated from apatite, Ca and Si from wollastonite, Al from corundum, Pb from galena, Th from ThO_2, and U from UO_2. Thorium, U, Pb, Y, and P were measured with LPET (large PET), and REE with LLIF (large LIF) and Si, Al with TAP analyzing crystal. The beam diameter was typically 3–5 μm. These conditions represent a suitable compromise between the degree of devastation of the measured spot, reaching high enough counting rates and the stability of the absorbed current.

The measurement is complicated by the presence of various interferences among the X-ray lines. We are using $ThM\alpha_1$, $UM\beta_1$, $PbM\alpha_1$, and $YL\alpha$ X-ray lines. The interferences between $PbM\alpha_1 - YL\gamma_1$ and $UM\alpha_1 - ThM\beta_1$ were corrected by empirically measured correction coefficients. Interferences between REE X-ray lines were also corrected, but these have no impact on the monazite dating. The fundamental requirements for monazite dating are very precise measurements of Pb, Th, U, and Y. The accuracy of monazite dating is therefore related to the monazite standards, whose variability is constrained by SHRIMP analyses. We are using the following age monazite standards: granite from Veikola, Finnland (1825 Ma), pegmatite from Madagascar (495 Ma), gneiss-migmatite from Dürstein/Wachau, Austria (341 Ma), granite from Aalfang, Austria (327 Ma) and monzogranite from Nakane, Japan (77 Ma). Before measuring monazites of unknown age we first measure all age monazite standards, each at least with 20 points. The ± 5–7 Ma deviations from the age for the each monazite age standards are considered as a good precision.

The statistical approach of Montel et al. (1996) was applied for the resulting age determination. The DAMON program was used for the age recalculations, histograms, and isochron plots (Konečný et al. 2004).

4. RESULTS

4.1. Parental rocks and monazite occurrences

Studied parental biotite granodiorites to muscovite-biotite monzogranites (Table 1, Fig. 2) show equigranular granitic, locally slightly porphyric texture. Plagioclase is the most common rock-forming mineral; it forms subhedral to euhedral crystals with polysynthetic albite-twinning, partly replaced by fine-lamellar muscovite ("sericite"), locally with albite rims. K-feldspar occurs as anhedral to euhedral crystals, with large porphyric individuals showing microperthitic or polysynthetic microcline lamellae

Tab. 1. Modal analyses of the studied rocks (without coarse-grained granitic pegmatites) of the Bratislava Massif (vol.%).

Rock	granodiorite	monzogranite	granodiorite	granodiorite	granodiorite	monzogranite	monzogranite	granodiorite	granodiorite	paragneiss
Locality	Devín	Devín	Bratislava	Devín	Rača	Borinka	Svätý Jur	Devín	Pezinok	Limbach
Sample	BMG-1	BMG-2	BMG-3	BMG-51	MK-6	MK-26	MK-58	MK-66	SMG-2	BMM-41
Quartz	30.4	23.7	39.5	37.4	38.2	39.3	31.0	34.3	36.4	43.2
Plagioclase	44.5	35.2	46.8	40.9	40.6	34.5	32.8	37.8	41.3	38.3
K-feldspar	11.5	31.0	5.5	14.8	10.1	20.4	28.2	18.5	17.8	-
Biotite	12.4	9.5	6.1	3.4	9.4	3.2	4.6	8.1	3.9	13.2
Muscovite	0.3	0.1	0.8	3.0	0.7	1.8	2.3	0.3	0.2	0.5
Garnet	-	-	-	-	-	-	-	-	-	0.3
Chlorite	-	-	-	-	-	-	-	-	-	3.7
Accessories	0.9	0.5	1.3	0.6	1.0	0.8	1.1	1.0	0.4	0.8
Point count	2500	2500	2500	2510	2268	2205	2182	2173	2500	2500
Q	35.2	26.4	43.0	40.2	43.0	41.7	33.7	37.9	38.1	-
A	13.3	34.5	6.0	15.9	11.4	21.7	30.7	20.4	18.6	-
P	51.5	39.1	51.0	43.9	45.6	36.6	35.6	41.7	43.3	-

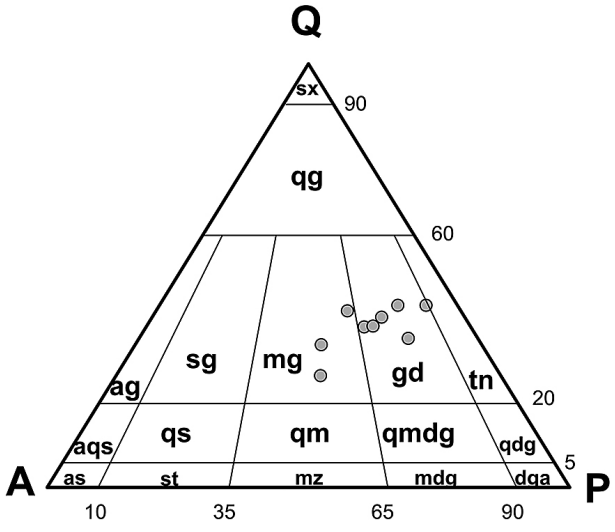

Fig. 2. QAP diagram of the studied granodiorites (gd) and monzogranites (mg) of the Bratislava Massif (vol.%).

patterns in some places. Euhedral plagioclase, rarely also biotite and quartz inclusions were identified in the K-feldspar. Quartz shows anhedral grains with undulatory extinction in association with the feldspars and micas; locally euhedral hexagonal crystals as inclusions in large K-feldspar phenocrysts were described (BMG-2 biotite monzogranite, Devín quarry). Biotite forms subhedral platy crystals in association with quartz, feldspar and muscovite or as euhedral pseudohexagonal crystal inclusions in K-feldspar phenocrysts. Subhedral muscovite forms late-magmatic inclusions in plagioclase; interstitial crystals or it partly replaced primary biotite. Accessory minerals include garnet (almandine > spessartine s.s.), apatite, zircon, monazite-(Ce), rarely xenotime-(Y), and opaque minerals (mainly ilmenite, magnetite, rutile, and pyrite).

Both granitic pegmatites samples (BMP-3 and BMP-21 samples) represent coarse-grained to blocky microcline-albite-quartz assemblages with muscovite, annite, accessory beryl, almandine-spessartine, zircon, monazite-(Ce), and occasionally gahnite (BMP-21).

For comparison to monazite from the granites and pegmatites, one sample of adjacent metapelite-metapsammite rock of the Pezinok Group was also studied. The garnet-(staurolite)-bearing chlorite-biotite paragneiss (the BMM-41 sample) shows a typical lepidogranoblastic texture with quartz-plagioclase- and biotite-rich parallel bands and porphyroblasts of almandine, rarely poikilitic staurolite (up to 15 mm) and presence of magnesian chlorite (clinochlore), muscovite and accessory ilmenite, zircon, apatite, and monazite-(Ce).

4.2. Monazite zoning and composition

Monazite forms scattered euhedral to subhedral crystals, usually 10 to 200 μm across, associating with quartz, feldspars, biotite, and zircon, usually in their interstices (Fig. 3A-B). The BSE images and EMPA of the granitic rocks show a relatively homogeneous pattern of monazite without distinct internal zoning (Fig. 3-D). By contrast, monazites from the Rössler quarry pegmatites and locally also from the paragneiss reveal a sector zoning caused by Th,U,Si,(Ca)- versus REE,Y,P-enriched and depleted sectors/zones, respectively (Fig. 3E-G).

Monazite-(Ce) crystals show compositions with Ce > La > Nd >> Sm,Y,HREE, exceptionally Ce > Nd > La >> Sm,Y,HREE abundances for all investigated samples (Table 2) and distinctive negative Eu anomaly in a chondrite-normalized diagram (Fig. 4). Both huttonite $ThSiREE_{-1}P_{-1}$ and cheralite $CaThREE_{-2}$ substitutions are recorded. The huttonite substitution is important in monazite of the granitic rocks, especially from the Devín quarry, whereas cheralite substitution is characteristic in both pegmatite samples (Rössler quarry and Dúbravka) and paragneiss from Limbach (Fig. 5A-C, 6). Some monazite crystals from the BGM granites show zones enriched in Th (up to ~ 9 wt. % ThO_2; ~ 0.09 apfu), whereas monazite from

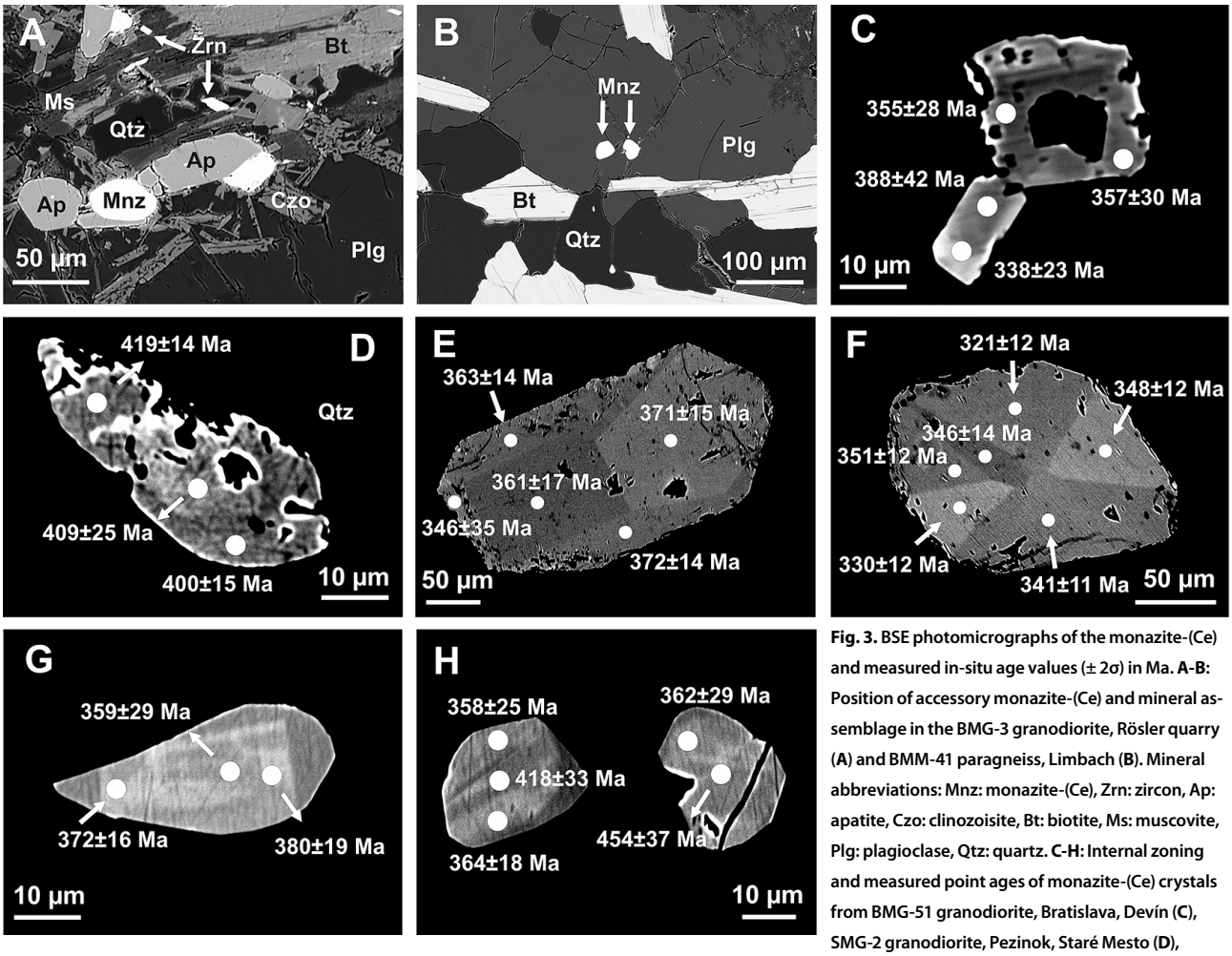

Fig. 3. BSE photomicrographs of the monazite-(Ce) and measured in-situ age values (± 2σ) in Ma. **A-B:** Position of accessory monazite-(Ce) and mineral assemblage in the BMG-3 granodiorite, Rösler quarry (**A**) and BMM-41 paragneiss, Limbach (**B**). Mineral abbreviations: Mnz: monazite-(Ce), Zrn: zircon, Ap: apatite, Czo: clinozoisite, Bt: biotite, Ms: muscovite, Plg: plagioclase, Qtz: quartz. **C-H:** Internal zoning and measured point ages of monazite-(Ce) crystals from BMG-51 granodiorite, Bratislava, Devín (**C**), SMG-2 granodiorite, Pezinok, Staré Mesto (**D**), BMP-3 granitic pegmatite, Bratislava, Rössler quarry (**E, F**), and BMM-41 paragneiss, Limbach, Slnečné Valley (**G, H**).

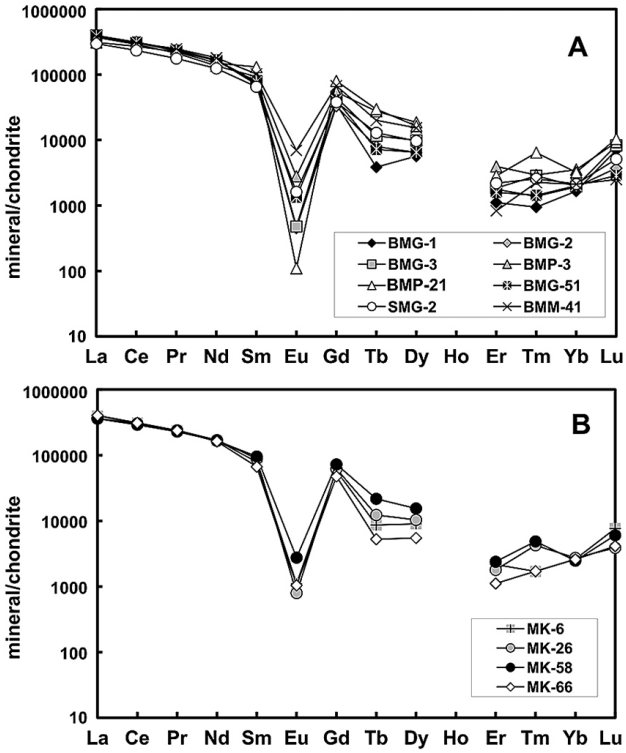

Fig. 4. A-B: Chondrite-normalized diagrams of monazite-(Ce) from the Bratislava Massif.

granitic pegmatites are commonly rich in U (up to ~ 4 wt. % UO_2; ~ 0.04 apfu); Table 2.

4.3. Monazite age

The investigated samples of the BGM and adjacent paragneiss gave two principal age populations: (i) dominant Hercynian, Lower Mississippian or Tournaisian ages (~ 360 to 350 Ma), and (ii) pre-Hercynian, Cambrian to Middle Devonian ages (~ 510 to 390 Ma), Table 3. The Hercynian age population displays a relatively narrow age interval for the granitic rocks and pegmatites: 359 ± 9 to 346 ± 10 Ma (Table 4). The same age is also revealed also by the staurolite-bearing paragneiss (359 ± 11 Ma). The measured Hercynian isochron ages of granites and pegmatites, (without the BMM-41 paragneiss sample) gave an average age of 353 ± 2 Ma (MSWD = 0.88, n = 290) – Table 4, Fig. 7A-B.

The older, pre-Hercynian ages in studied samples from monazite of the BGM granites and paragneiss show distribution intervals at 420–400 Ma (n = 20), 470–430 Ma (n = 13),

Tab. 2. Representative compositions of monazite-(Ce) from the Bratislava Massif (wt.%).

Sample	BMG-1	BMG-2	BMG-3	BMP-3	BMG-51	SMG-2	BMM-41	MK-6	MK-26	MK-58
P_2O_5	27.76	27.46	27.35	29.43	29.30	29.19	29.49	28.60	28.60	29.16
As_2O_5	0.15	0.15	0.14	0.14	0.15	0.15	0.00	0.16	0.16	0.14
SiO_2	1.47	1.02	1.25	0.16	0.40	0.42	0.21	0.56	0.22	0.21
ThO_2	7.05	6.29	9.30	2.54	4.94	5.64	3.21	4.38	5.43	5.27
UO_2	0.25	0.09	0.18	4.26	0.31	0.22	0.52	0.14	0.60	1.47
Al_2O_3	0.12	0.00	0.00	0.00	0.01	0.00	0.00	0.00	0.00	0.00
Y_2O_3	1.13	0.50	0.53	2.33	1.46	1.71	1.78	1.11	1.97	1.86
La_2O_3	12.24	15.72	15.48	13.45	12.80	11.54	14.12	14.57	12.64	13.44
Ce_2O_3	28.94	30.64	28.34	27.76	28.68	27.81	28.78	30.37	28.01	27.54
Pr_2O_3	3.42	3.11	2.81	2.95	3.21	3.27	3.31	3.29	3.13	2.94
Nd_2O_3	12.51	11.37	9.69	9.46	12.19	12.68	12.39	11.70	11.70	10.79
Sm_2O_3	2.10	1.41	1.17	2.40	2.38	2.60	2.13	1.68	2.18	2.09
Eu_2O_3	0.05	0.00	0.00	0.03	0.05	0.00	0.11	0.00	0.00	0.04
Gd_2O_3	1.41	0.87	0.74	1.57	1.79	2.13	1.98	1.76	2.12	2.17
Tb_2O_3	0.09	0.00	0.03	0.11	0.07	0.09	0.11	0.08	0.15	0.16
Dy_2O_3	0.35	0.07	0.16	0.77	0.43	0.54	0.70	0.25	0.60	0.56
Ho_2O_3	0.19	0.28	0.18	0.11	0.17	0.13	0.15	0.12	0.12	0.16
Er_2O_3	0.00	0.00	0.08	0.15	0.02	0.00	0.06	0.01	0.00	0.17
Tm_2O_3	0.00	0.00	0.00	0.00	0.03	0.00	0.00	0.03	0.00	0.00
Yb_2O^3	0.03	0.00	0.10	0.03	0.09	0.14	0.00	0.00	0.13	0.12
Lu_2O_3	0.00	0.00	0.06	0.00	0.00	0.15	0.00	0.00	0.00	0.00
CaO	0.78	0.56	1.35	1.37	1.00	1.01	0.79	0.76	1.22	1.46
PbO	0.13	0.11	0.15	0.24	0.09	0.11	0.10	0.07	0.12	0.17
Total	100.16	99.64	99.08	99.25	99.58	99.51	99.94	99.62	99.11	99.90
Formulae based on 4 oxygen atoms										
P	0.935	0.940	0.937	0.985	0.979	0.978	0.984	0.965	0.970	0.976
As	0.003	0.003	0.003	0.003	0.003	0.003	0.000	0.003	0.003	0.003
Si	0.058	0.041	0.051	0.006	0.016	0.016	0.008	0.022	0.009	0.008
Th	0.064	0.058	0.086	0.023	0.044	0.051	0.029	0.040	0.050	0.047
U	0.002	0.001	0.002	0.037	0.003	0.002	0.005	0.001	0.005	0.013
Al	0.005	0.000	0.000	0.000	0.001	0.000	0.000	0.000	0.000	0.000
Y	0.024	0.011	0.011	0.049	0.031	0.036	0.037	0.023	0.042	0.039
La	0.180	0.234	0.231	0.196	0.186	0.168	0.205	0.214	0.187	0.196
Ce	0.422	0.454	0.420	0.402	0.415	0.403	0.415	0.443	0.411	0.399
Pr	0.050	0.046	0.041	0.043	0.046	0.047	0.048	0.048	0.046	0.042
Nd	0.178	0.164	0.140	0.134	0.172	0.179	0.174	0.167	0.167	0.152
Sm	0.029	0.020	0.016	0.033	0.032	0.035	0.029	0.023	0.030	0.028
Eu	0.001	0.000	0.000	0.000	0.001	0.000	0.001	0.000	0.000	0.000
Gd	0.019	0.012	0.010	0.021	0.023	0.028	0.026	0.023	0.028	0.028
Tb	0.001	0.000	0.000	0.001	0.001	0.001	0.001	0.001	0.002	0.002
Dy	0.005	0.001	0.002	0.010	0.005	0.007	0.009	0.003	0.008	0.007
Ho	0.002	0.004	0.002	0.001	0.002	0.002	0.002	0.001	0.002	0.002
Er	0.000	0.000	0.001	0.002	0.000	0.000	0.001	0.000	0.000	0.002
Tm	0.000	0.000	0.000	0.000	0.000	0.000	0.000	0.000	0.000	0.000
Yb	0.000	0.000	0.001	0.000	0.001	0.002	0.000	0.000	0.002	0.001
Lu	0.000	0.000	0.001	0.000	0.000	0.002	0.000	0.000	0.000	0.000

Ca	0.033	0.024	0.059	0.058	0.042	0.043	0.033	0.032	0.053	0.062
Pb	0.001	0.001	0.002	0.003	0.001	0.001	0.001	0.001	0.001	0.002
Total	**2.012**	**2.014**	**2.015**	**2.007**	**2.006**	**2.005**	**2.009**	**2.012**	**2.015**	**2.013**

Tab. 3. Analytical data and ages of monazite-(Ce) from the studied samples, the Bratislava Massif. [1]

Sample#	Th wt.%	U wt.%	Pb wt.%	Y wt.%	Age (Ma)	Age 2σ
BMG-1	5.337	0.069	0.095	0.293	365	25.5
BMG-1	5.027	0.081	0.086	0.302	348	26.5
BMG-1	6.132	0.108	0.093	0.354	308	21.7
BMG-1	5.857	0.113	0.103	0.449	355	22.9
BMG-1	6.337	0.358	0.103	1.298	300	19.1
BMG-1	6.088	0.148	0.106	0.624	349	21.7
BMG-1	4.041	0.049	0.069	0.310	344	33.3
BMG-1	5.483	0.116	0.086	0.511	314	23.8
BMG-1	5.665	0.306	0.121	1.549	398	22.2
BMG-1	6.200	0.217	0.110	0.893	347	20.8
BMG-1	6.183	0.324	0.163	1.259	493	21.4
BMG-1	4.299	0.064	0.075	0.374	352	30.7
BMG-1	4.799	0.077	0.090	0.363	380	27.9
BMG-1	4.770	0.078	0.087	0.371	370	27.9
BMG-1	4.791	0.085	0.081	0.475	338	27.5
BMG-1	5.786	0.113	0.104	0.433	362	23.0
BMG-1	6.316	0.116	0.105	0.553	338	21.4
BMG-1	5.331	0.094	0.092	0.398	350	24.9
BMG-1	5.609	0.134	0.096	0.745	343	23.3
BMG-1	5.443	0.123	0.086	0.625	316	23.9
BMG-1	4.816	0.109	0.078	0.562	320	26.8
BMG-1	4.750	0.077	0.057	0.327	237	26.7
BMG-1	5.368	0.091	0.086	0.432	322	24.7
BMG-2	4.882	0.200	0.096	0.607	371	25.5
BMG-2	5.129	0.075	0.087	0.392	344	26.0
BMG-2	4.590	0.158	0.087	0.637	364	27.5
BMG-2	4.691	0.141	0.083	0.613	346	27.1
BMG-2	6.670	0.128	0.109	0.414	331	20.2
BMG-2	4.733	0.088	0.082	0.356	348	27.9
BMG-2	5.528	0.083	0.090	0.392	330	24.2
BMG-2	5.125	0.126	0.097	0.644	377	25.6
BMG-2	5.499	0.118	0.089	0.548	325	23.8
BMG-2	6.326	0.114	0.106	0.473	340	21.3
BMG-2	5.272	0.172	0.096	0.544	353	24.2
BMG-2	5.306	0.106	0.080	0.433	303	24.5
BMG-2	5.375	0.076	0.081	0.402	307	24.5
BMG-2	5.591	0.079	0.093	0.311	341	24.1
BMG-2	4.727	0.074	0.081	0.324	346	28.1
BMG-2	4.719	0.083	0.086	0.383	368	28.2
BMG-2	4.733	0.088	0.082	0.356	348	27.9
BMG-2	5.528	0.083	0.090	0.392	330	24.2
BMG-2	5.125	0.126	0.097	0.644	377	25.6

Sample#	Th wt.%	U wt.%	Pb wt.%	Y wt.%	Age (Ma)	Age 2σ
BMG-2	5.499	0.118	0.089	0.548	325	23.8
BMG-2	6.326	0.114	0.106	0.473	340	21.3
BMG-2	5.272	0.172	0.096	0.544	353	24.2
BMG-2	5.306	0.106	0.080	0.433	303	24.5
BMG-2	5.375	0.076	0.081	0.402	307	24.5
BMG-2	5.591	0.079	0.093	0.311	341	24.1
BMG-2	4.727	0.074	0.081	0.324	346	28.1
BMG-2	4.719	0.083	0.086	0.383	368	28.2
BMG-2	4.979	0.149	0.086	0.754	337	25.6
BMG-2	5.779	0.137	0.098	0.603	340	22.8
BMG-2	5.381	0.393	0.106	1.745	349	21.5
BMG-2	6.299	0.211	0.110	0.944	341	20.5
BMG-2	6.229	0.201	0.103	0.844	325	20.8
BMG-2	4.779	0.126	0.077	0.768	317	26.8
BMG-2	4.753	0.082	0.093	0.478	395	28.2
BMG-2	5.135	0.112	0.093	0.680	364	25.7
BMG-2	5.258	0.118	0.092	0.621	350	25.2
BMG-2	4.558	0.095	0.081	0.522	356	28.8
BMG-2	5.666	0.116	0.099	0.521	350	23.3
BMG-2	5.654	0.144	0.102	0.653	360	23.1
BMG-2	5.355	0.086	0.091	0.402	345	25.1
BMG-2	5.980	0.111	0.103	0.606	350	22.6
BMG-3	5.160	0.131	0.089	0.513	358	25.1
BMG-3	4.526	0.196	0.086	0.659	374	27.2
BMG-3	5.371	0.111	0.094	0.443	367	24.7
BMG-3	4.509	0.121	0.089	0.508	406	29.1
BMG-3	6.610	0.108	0.114	0.482	365	20.8
MG-3	5.915	0.100	0.109	0.468	390	23.1
BMG-3	8.169	0.158	0.136	0.418	349	16.9
BMG-3	5.903	0.222	0.099	0.799	335	21.4
BMG-3	3.662	0.105	0.072	0.469	399	35.3
BMG-3	4.355	0.827	0.114	1.796	363	20.6
BMG-3	4.055	0.537	0.098	1.454	378	24.5
BMG-3	5.815	0.092	0.101	0.450	368	23.3
BMG-3	4.499	0.658	0.127	1.594	427	22.2
BMG-3	3.908	0.358	0.083	1.366	366	27.9
BMG-3	3.419	0.126	0.073	0.511	428	36.8
BMG-3	3.556	0.290	0.092	1.226	455	31.9
BMG-3	3.790	0.489	0.090	1.403	373	26.3
BMG-3	4.167	0.564	0.097	1.623	361	24.0
BMG-3	4.212	0.117	0.077	0.366	376	30.4
BMG-3	3.816	0.088	0.066	0.346	362	33.6

Tab. 3. Analytical data and ages of monazite-(Ce) from the studied samples. the Bratislava Massif. [2]

Sample#	Th wt.%	U wt.%	Pb wt.%	Y wt.%	Age (Ma)	Age 2σ
BMG-3	4.435	0.668	0.104	1.530	353	19.1
BMG-3	5.049	0.165	0.091	0.859	366	22.3
BMG-3	4.393	0.621	0.096	1.577	336	19.6
BMG-3	5.220	0.168	0.085	0.674	332	21.4
BMG-3	4.422	0.122	0.077	0.442	356	25.7
BMG-3	4.183	0.315	0.113	1.189	484	24.8
BMG-3	4.115	0.561	0.091	1.532	344	21.1
BMG-3	5.746	0.142	0.086	0.551	309	19.8
BMG-3	4.403	0.575	0.098	1.532	351	20.0
BMG-3	4.818	0.100	0.089	0.477	387	27.4
BMG-3	5.611	0.195	0.091	0.759	325	22.7
BMG-3	4.281	0.677	0.101	1.636	351	22.1
BMG-3	3.980	0.474	0.096	1.432	389	25.8
BMG-3	5.353	0.162	0.073	0.436	277	23.1
BMG-3	5.331	0.164	0.095	0.623	361	23.9
BMG-3	4.282	0.438	0.092	1.405	359	24.7
BMG-3	3.861	0.695	0.093	1.632	339	23.0
BMG-3	4.576	0.116	0.081	0.646	366	28.3
BMG-3	4.261	0.093	0.080	0.580	389	30.8
BMG-3	4.301	0.743	0.099	1.663	329	21.3
BMP-3	3.585	1.485	0.139	1.902	369	17.4
BMP-3	3.658	1.367	0.130	1.837	360	17.9
BMP-3	2.935	1.448	0.120	1.974	354	19.0
BMP-3	3.810	1.621	0.142	2.203	351	16.2
BMP-3	3.640	1.776	0.153	1.910	365	15.8
BMP-3	4.293	1.843	0.174	1.834	378	14.6
BMP-3	3.408	1.730	0.151	1.919	374	16.5
BMP-3	3.437	1.594	0.137	1.693	356	16.8
BMP-3	3.376	1.465	0.131	1.540	361	17.7
BMP-3	4.038	2.199	0.180	2.127	361	13.4
BMP-3	4.399	2.057	0.165	2.468	334	13.6
BMP-3	2.370	2.358	0.150	2.402	336	14.7
BMP-3	2.834	2.245	0.164	1.962	363	14.7
BMP-3	2.213	3.346	0.204	1.698	350	11.7
BMP-3	2.234	3.752	0.217	1.832	339	10.7
BMP-3	1.905	3.517	0.207	2.085	348	11.5
BMP-3	1.776	2.860	0.171	1.681	347	13.5
BMP-3	2.336	3.921	0.245	2.226	364	10.4
BMP-3	2.305	3.570	0.224	1.718	361	11.1
BMP-3	2.135	3.189	0.193	2.229	348	12.2
BMP-3	2.923	3.278	0.206	2.600	341	11.3
BMP-3	2.439	3.337	0.195	2.211	330	11.5
BMP-3	2.152	3.126	0.192	2.728	351	12.4
BMP-3	3.057	2.264	0.160	2.834	346	14.4
BMP-3	2.370	3.365	0.190	2.616	321	11.5
BMP-3	4.072	1.781	0.163	1.899	371	15.2
BMP-3	3.675	1.508	0.138	1.762	361	17.1

Sample#	Th wt.%	U wt.%	Pb wt.%	Y wt.%	Age (Ma)	Age 2σ
BMP-3	4.336	1.899	0.174	2.215	372	14.3
BMP-3	4.245	1.943	0.171	2.272	363	14.3
BMP-3	3.354	0.166	0.060	0.781	346	35.3
BMP-21	5.010	2.140	0.180	1.710	339	13.7
BMP-21	5.430	1.153	0.157	0.319	382	17.4
BMP-21	5.268	1.478	0.137	1.255	306	15.7
BMP-21	3.486	2.337	0.167	1.766	339	14.5
BMP-21	4.905	2.153	0.190	1.801	358	13.8
BMP-21	5.069	1.422	0.154	0.479	356	16.5
BMP-21	4.823	1.373	0.153	0.445	370	17.1
BMP-21	5.265	1.039	0.133	0.224	345	18.1
BMP-21	5.312	1.115	0.137	0.799	344	17.5
BMP-21	4.243	1.289	0.134	0.961	357	18.6
BMP-21	7.988	1.714	0.219	0.577	361	12.3
BMP-21	5.907	2.043	0.199	1.925	356	13.2
BMP-21	4.316	2.339	0.191	2.101	359	13.9
BMP-21	4.251	2.585	0.200	1.973	355	13.0
BMP-21	4.993	2.679	0.231	1.948	377	12.3
BMP-21	5.550	3.409	0.273	2.168	368	10.5
BMP-21	2.946	3.453	0.230	2.026	364	11.9
BMP-21	5.262	2.000	0.197	1.743	375	14.0
BMP-21	4.159	1.690	0.133	1.733	311	15.9
BMP-21	5.112	1.671	0.182	1.023	387	15.5
BMG-51	5.231	1.351	0.139	1.186	324	15.1
BMG-51	4.340	0.270	0.080	1.152	342	26.8
BMG-51	3.514	0.156	0.067	0.725	373	34.7
BMG-51	3.308	0.144	0.058	1.009	343	36.5
BMG-51	4.057	0.090	0.083	0.419	426	32.3
BMG-51	3.853	0.164	0.082	0.622	418	32.1
BMG-51	4.226	0.175	0.077	1.327	357	29.6
BMG-51	2.901	0.128	0.067	0.499	448	42.0
BMG-51	2.879	0.118	0.057	0.515	388	42.3
BMG-51	5.739	0.150	0.094	0.770	338	22.7
BMG-51	4.851	0.065	0.080	0.307	355	27.6
BMG-51	3.775	0.091	0.071	0.431	390	34.1
BMG-51	2.852	0.122	0.048	0.683	332	41.9
BMG-51	4.492	0.198	0.080	1.207	350	27.1
BMG-51	5.460	0.083	0.092	0.362	360	24.6
BMG-51	6.191	0.138	0.092	0.558	310	21.2
BMG-51	5.726	0.086	0.108	0.629	401	23.8
BMG-51	6.171	0.079	0.109	0.535	377	22.2
BMG-51	5.908	0.095	0.105	0.533	376	23.0
BMG-51	5.084	0.060	0.089	0.449	378	26.5
SMG-2	4.693	0.064	0.090	0.404	411	29.0
SMG-2	5.948	0.118	0.111	0.523	391	22.8
SMG-2	4.658	0.086	0.086	0.379	388	28.6
SMG-2	5.154	0.216	0.085	0.694	326	24.0

Tab. 3. Analytical data and ages of monazite-(Ce) from the studied samples, the Bratislava Massif. [3]

Sample#	Th wt.%	U wt.%	Pb wt.%	Y wt.%	Age (Ma)	Age 2σ
SMG-2	5.204	0.165	0.105	1.054	409	24.9
SMG-2	5.650	1.376	0.181	1.633	400	14.9
SMG-2	5.643	1.549	0.200	1.585	419	14.3
SMG-2	4.952	0.228	0.114	1.346	445	25.5
SMG-2	4.841	0.758	0.151	1.446	461	20.2
SMG-2	4.962	0.128	0.080	0.423	332	25.8
SMG-2	5.192	0.970	0.155	1.672	414	17.8
SMG-2	6.416	0.804	0.158	1.165	392	16.5
SMG-2	5.370	0.911	0.156	1.463	418	17.8
SMG-2	5.666	0.326	0.124	1.311	412	21.6
SMG-2	5.338	0.529	0.145	1.874	457	21.1
SMG-2	5.100	0.135	0.093	0.531	376	25.6
SMG-2	5.120	1.042	0.165	1.236	432	17.6
SMG-2	4.831	0.147	0.108	0.489	452	27.3
SMG-2	4.663	0.883	0.140	0.909	415	19.4
SMG-2	4.964	0.400	0.124	1.846	441	23.3
SMG-2	4.994	0.904	0.136	1.248	383	16.4
SMG-2	5.546	1.159	0.157	1.401	377	14.0
SMG-2	5.321	0.269	0.095	1.826	343	20.4
SMG-2	4.811	0.138	0.089	0.854	380	23.8
SMG-2	5.676	1.165	0.147	1.625	347	13.8
SMG-2	4.978	0.338	0.095	1.420	351	20.7
SMG-2	4.422	0.065	0.069	0.361	333	26.0
SMG-2	5.040	0.831	0.118	1.539	341	16.3
SMG-2	5.696	0.115	0.093	0.608	341	20.3
SMG-2	4.895	0.121	0.095	0.900	403	23.9
SMG-2	5.477	0.884	0.141	1.432	378	17.6
SMG-2	5.036	0.831	0.123	1.373	357	18.7
SMG-2	5.158	0.183	0.090	1.054	351	24.6
SMG-2	4.094	0.088	0.082	0.399	417	32.3
SMG-2	6.068	1.901	0.189	1.808	346	12.5
SMG-2	5.712	1.061	0.148	1.350	362	16.1
SMG-2	4.686	0.434	0.095	1.645	350	23.5
SMG-2	5.490	0.690	0.123	1.868	357	18.8
SMG-2	5.233	0.845	0.134	1.881	374	18.3
SMG-2	5.218	0.681	0.117	1.752	354	19.5
SMG-2	5.402	1.014	0.152	1.718	391	17.0
SMG-2	5.453	0.669	0.122	1.922	359	19.1
SMG-2	4.931	0.970	0.142	1.739	393	18
SMG-2	4.749	0.104	0.082	0.389	361	27.4
SMG-2	4.750	0.539	0.120	1.524	414	22.0
SMG-2	5.269	0.777	0.125	1.902	360	18.8
SMG-2	5.589	0.087	0.094	0.405	358	24.3
SMG-2	4.412	0.080	0.085	0.397	405	30.2
SMG-2	4.804	0.542	0.101	2.415	345	21.9
SMG-2	5.427	0.612	0.130	2.156	392	19.9
SMG-2	5.374	1.055	0.153	1.424	390	17.1
SMG-2	5.546	1.017	0.159	1.473	401	16.9
MK-6	3.849	0.124	0.057	0.871	300	32.3
MK-6	4.428	0.814	0.099	1.517	315	20.1
MK-6	3.949	0.546	0.075	1.496	293	24.3
MK-6	5.684	0.100	0.093	0.615	347	23.6
MK-6	4.338	0.248	0.082	1.271	357	27.4
MK-6	4.839	0.189	0.084	0.931	344	25.9
MK-6	4.945	0.252	0.093	0.952	360	24.8
MK-6	4.732	0.130	0.078	0.853	340	27.3
MK-6	5.645	0.143	0.087	0.680	320	23.0
MK-6	5.519	0.104	0.094	0.559	358	24.2
MK-6	3.639	0.268	0.068	0.974	340	30.8
MK-6	4.690	0.105	0.078	0.438	345	27.7
MK-6	4.676	0.312	0.094	1.204	368	25.2
MK-6	5.862	0.137	0.110	1.093	390	22.9
MK-6	3.517	0.307	0.082	1.224	403	31.2
MK-6	3.281	0.057	0.052	0.705	333	39.2
MK-6	4.501	0.160	0.079	1.157	353	27.9
MK-6	4.336	0.105	0.077	0.826	368	30.0
MK-6	4.327	0.272	0.078	1.204	333	26.8
MK-6	4.363	0.099	0.082	0.549	391	30.0
MK-6	3.959	0.163	0.076	0.920	380	31.5
MK-6	3.668	0.121	0.070	0.952	384	34.4
MK-26	4.547	0.382	0.101	1.394	388	24.7
MK-26	4.772	0.529	0.104	1.550	359	22.0
MK-26	4.977	0.073	0.085	0.213	363	26.9
MK-26	4.085	0.601	0.093	1.806	346	23.4
MK-26	4.086	0.749	0.083	2.035	285	21.3
MK-26	5.239	0.153	0.091	0.873	353	24.6
MK-26	5.651	0.194	0.091	1.130	325	22.4
MK-26	5.692	0.141	0.106	0.917	385	23.4
MK-26	5.290	0.116	0.091	0.851	360	25.1
MK-26	5.709	0.199	0.100	1.061	352	22.4
MK-26	5.537	0.284	0.098	1.251	340	22.0
MK-26	5.490	0.199	0.099	1.200	362	23.2
MK-26	5.474	0.147	0.093	0.863	350	23.7
MK-26	5.257	0.159	0.098	0.849	379	24.7
MK-26	5.928	0.136	0.106	0.784	373	22.6
MK-26	5.796	0.135	0.103	0.784	371	23.2
MK-26	5.241	0.118	0.092	0.744	364	25.2
MK-26	4.903	0.103	0.083	0.713	356	26.9
MK-26	5.563	0.172	0.121	0.862	439	23.8
MK-26	5.489	0.130	0.089	0.852	336	23.7
MK-26	5.074	0.118	0.087	0.748	354	25.8
MK-26	5.225	0.104	0.090	0.748	360	25.4
MK-26	4.617	0.159	0.079	1.008	343	27.3
MK-26	3.857	0.102	0.067	0.796	360	33.1

Tab. 3. Analytical data and ages of monazite-(Ce) from the studied samples, the Bratislava Massif. [4]

Sample#	Th wt.%	U wt.%	Pb wt.%	Y wt.%	Age (Ma)	Age 2σ
MK-26	4.066	0.089	0.057	0.601	291	31.3
MK-26	5.275	0.113	0.100	0.835	395	25.4
MK-26	5.310	0.091	0.080	0.422	319	25.0
MK-26	5.455	0.132	0.086	0.810	329	23.8
MK-26	4.097	0.089	0.076	0.697	385	31.8
MK-26	3.756	0.084	0.070	0.725	390	34.7
MK-26	4.546	0.084	0.089	0.645	414	29.5
MK-26	3.674	0.230	0.087	0.955	437	32.1
MK-26	3.240	0.553	0.084	1.410	373	27.7
MK-26	3.959	0.427	0.087	1.627	363	26.5
MK-26	5.083	0.128	0.088	0.550	360	25.7
MK-26	4.229	0.116	0.068	0.490	329	30.1
MK-26	4.427	0.073	0.071	0.342	338	29.5
MK-58	3.455	0.463	0.076	2.325	343	28.4
MK-58	4.634	1.294	0.144	1.463	365	16.7
MK-58	3.969	0.809	0.106	1.709	359	21.7
MK-58	3.186	0.550	0.075	0.735	340	27.7
MK-58	4.545	0.430	0.089	2.044	337	23.9
MK-58	5.144	0.377	0.095	1.133	335	22.2
MK-58	4.177	0.366	0.088	1.546	365	26.2
MK-58	4.900	0.348	0.105	1.108	388	23.9
MK-58	4.393	0.166	0.080	0.661	364	28.7
MK-58	4.150	0.152	0.075	0.840	362	30.0
MK-58	4.884	0.292	0.086	1.025	329	24.0
MK-58	3.712	0.329	0.075	2.001	353	29.2
MK-58	3.745	0.415	0.082	2.071	361	27.6
MK-58	3.765	0.254	0.070	1.550	343	30.2
MK-58	3.943	0.306	0.081	2.208	366	28.7
MK-58	3.665	0.407	0.083	2.213	373	28.3
MK-58	3.620	1.297	0.133	1.999	379	18.7
MK-58	3.633	0.359	0.078	2.090	365	29.5
MK-58	3.804	0.395	0.082	2.189	361	27.7
MK-58	2.997	0.399	0.071	1.769	372	32.6
MK-58	4.533	0.145	0.074	0.663	331	27.8
MK-58	4.969	0.147	0.085	0.670	351	25.8
MK-58	4.553	0.123	0.078	0.666	352	28.4
MK-58	5.243	0.165	0.093	0.696	358	24.5
MK-58	5.118	0.168	0.084	0.682	330	24.8
MK-58	8.684	0.304	0.146	0.996	338	15.2
MK-58	4.984	0.340	0.091	1.055	335	23.3
MK-58	3.967	0.373	0.078	1.160	336	27.0
MK-58	3.061	0.426	0.076	0.655	383	31.5
MK-58	2.399	0.038	0.044	0.348	391	45.0
MK-58	4.972	0.199	0.099	0.425	395	25.2
MK-58	4.170	0.141	0.084	0.392	405	30.2
MK-58	4.153	0.673	0.095	2.431	338	22.5
MK-58	4.111	0.581	0.106	2.011	394	24.0
MK-58	4.539	0.163	0.080	1.010	354	27.7
MK-58	4.613	0.290	0.101	1.875	405	26.0
MK-58	3.656	1.023	0.104	1.497	336	20.3
MK-58	1.952	0.404	0.049	0.590	339	41.8
MK-58	2.013	0.605	0.073	0.653	408	34.8
MK-58	3.687	1.282	0.112	1.741	320	18.1
MK-58	3.836	0.457	0.090	2.067	380	26.8
MK-58	3.315	0.694	0.081	1.907	327	25.3
MK-58	3.220	0.715	0.090	1.858	363	25.5
MK-58	3.598	0.649	0.089	1.749	349	24.8
MK-66	6.465	0.189	0.117	0.728	369	20.5
MK-66	4.796	0.056	0.085	0.377	382	28.4
MK-66	5.683	0.076	0.101	0.320	380	24.3
MK-66	5.470	0.093	0.095	0.387	368	24.6
MK-66	5.887	0.105	0.103	0.479	368	23.0
MK-66	4.409	0.065	0.101	0.264	488	31.8
MK-66	6.044	0.146	0.098	0.679	336	21.8
MK-66	3.689	0.061	0.060	0.368	344	35.5
MK-66	4.858	0.098	0.078	0.464	337	27.1
MK-66	5.377	0.115	0.131	0.446	506	26.2
MK-66	5.358	0.112	0.087	0.401	339	24.5
MK-66	4.985	0.074	0.093	0.351	397	27.1
MK-66	5.742	0.091	0.095	0.403	351	23.4
MK-66	5.419	0.078	0.086	0.366	338	24.8
MK-66	4.266	1.098	0.123	1.734	352	18.7
MK-66	4.507	0.079	0.069	0.639	325	29.0
MK-66	5.153	0.080	0.087	0.752	361	26.0
MK-66	6.187	0.137	0.096	0.687	325	21.5
MK-66	6.136	0.156	0.099	0.636	333	21.4
MK-66	4.830	0.076	0.082	0.365	361	27.6
MK-66	4.415	0.081	0.082	0.323	392	30.2
MK-66	5.368	0.081	0.087	0.464	346	24.9
MK-66	6.172	0.203	0.106	0.986	346	21.1
MK-66	5.266	0.072	0.088	0.343	359	25.7
MK-66	5.918	0.087	0.098	0.330	354	23.1
MK-66	4.804	0.077	0.084	0.328	373	27.7
MK-66	5.951	0.087	0.088	0.325	314	22.8
MK-66	5.637	0.129	0.100	0.591	368	23.6
MK-66	5.938	0.134	0.102	0.618	358	22.5
MK-66	4.854	0.109	0.081	0.426	348	27.0
MK-66	6.050	0.164	0.102	0.643	346	21.7
BMM-41	2.751	0.460	0.067	1.429	355	32.9
BMM-41	1.658	0.524	0.057	1.329	382	41.0
BMM-41	2.740	0.582	0.074	1.445	357	30.2
BMM-41	2.075	0.682	0.064	1.548	337	32.3
BMM-41	1.876	0.471	0.064	1.466	419	41.1
BMM-41	2.348	0.443	0.059	1.138	351	36.2

Tab. 3. Analytical data and ages of monazite-(Ce) from the studied samples, the Bratislava Massif. [5]

Sample#	Th wt.%	U wt.%	Pb wt.%	Y wt.%	Age (Ma)	Age 2σ
BMM-41	3.123	0.513	0.083	1.361	386	29.5
BMM-41	3.445	0.721	0.083	1.592	323	24.4
BMM-41	2.836	0.424	0.063	1.279	334	32.6
BMM-41	2.269	0.473	0.077	1.337	454	37.1
BMM-41	2.496	0.485	0.072	1.327	394	34.2
BMM-41	1.938	0.447	0.056	0.198	373	35.8
BMM-41	2.960	0.608	0.072	1.352	329	24.8
BMM-41	3.376	1.039	0.110	0.104	364	18.5
BMM-41	2.031	0.512	0.069	0.058	418	32.9
BMM-41	2.540	0.748	0.079	0.179	358	24.6
BMM-41	1.936	0.418	0.067	0.153	454	37.2
BMM-41	2.361	0.583	0.069	0.182	362	29.0
BMM-41	4.447	1.156	0.136	0.167	372	15.8
BMM-41	2.630	0.430	0.064	0.205	359	29.2
BMM-41	4.497	0.622	0.111	0.240	380	19.1
BMM-41	2.144	0.438	0.063	1.325	394	34.3
BMM-41	3.215	0.865	0.096	1.775	359	20.9
BMM-41	3.712	0.834	0.096	1.749	335	19.5
BMM-41	2.410	0.444	0.063	1.376	367	31.7
BMM-41	2.165	0.394	0.042	1.398	276	34.7
BMM-41	2.823	0.460	0.080	1.404	415	28.7
BMM-41	2.284	0.403	0.054	1.361	337	33.5
BMM-41	3.023	0.503	0.077	1.348	371	26.3
BMM-41	2.341	0.482	0.078	1.556	447	32.1
BMM-41	2.710	0.355	0.060	1.283	351	31.4

Tab. 4. Results of electron microprobe dating of monazite-(Ce) from the studied samples: average ages of Hercynian monazite-(Ce) population (<380 Ma) for each locality and average ages of Hercynian and Pre-Hercynian populations of the whole Bratislava Massif.

Locality	Rock	Sample#	Average age (Ma)	Age 2σ (± Ma)	Number	MSWD
Bratislava, Devín	granodiorite	BMG-1	353	11	20	0.95
Bratislava, Devín	monzogranite	BMG-2	359	9	30	0.64
Bratislava, Rössler q.	granodiorite	BMG-3	359	8	34	0.65
Bratislava, Rössler q.	pegmatite	BMP-3	352	5	30	1.08
Bratislava, Dúbravka	pegmatite	BMP-21	357	6	20	1.87
Bratislava, Devín	granodiorite	BMG-51	353	14	14	0.72
Pezinok, Staré Mesto	granodiorite	SMG-2	354	8	23	0.52
Bratislava, Rača	granodiorite	MK-6	349	11	22	1.17
Borinka, Popálené	monzogranite	MK-26	357	9	32	0.59
Sv. Jur, Človečia Hlava	monzogranite	MK-58	353	7	43	0.57
Bratislava, Devín	granodiorite	MK-66	346	10	22	0.36
Limbach	paragneiss	BMM-41	359	11	24	0.54
Bratislava Massif: Average of Hercynian ages			353	2	290	0.88
Bratislava Massif: Average of Pre-Hercynian ages			420	7	45	1.05

and 500–490 Ma (n = 2), Fig. 8A. Younger data are very rare (~ 290 to 240 Ma, n = 5). The pre-Hercynian ages are irregularly distributed in some monazite crystals or their zones (Fig. 3D). They are generally scarce in majority of studied granitic rocks with an exception of the SMG-2 biotite granodiorite (Pezinok, Staré Mesto), where 37 % of measured spots gave ~ 400 Ma ages (Table 3, Fig. 3D). An average calculated isochron age of the pre-Hercynian monazite population gave 420±7 Ma (Table 4, Fig. 8B). A detailed comparative study of the electron-microprobe analyses revealed some compositional differences between the dominant ~ 350 Ma and the older monazite populations. Generally, the ~ 460 to ~ 400 Ma old monazite populations have commonly higher REE + Y + P + As and lower Th + U + Si contents, whereas the oldest ~ 505 to ~480 Ma population exhibits usually higher Th + U + Si and lower REE + Y + P + As contents in comparison to the ~ 350 Ma one (Table 2, Fig. 5C). The composition of the youngest, ~ 290–240 Ma old monazite population does not show any systematic differences in comparison to both the Hercynian and pre-Hercynian populations (Fig. 5C).

5. DISCUSSION AND CONCLUSIONS

5.1. Monazite composition

Accessory monazite is one of the main carriers of the rare-earth elements (REE) in granitic rocks, together with allanite-(Ce), and xenotime-(Y). Primary magmatic monazite-(Ce) is the

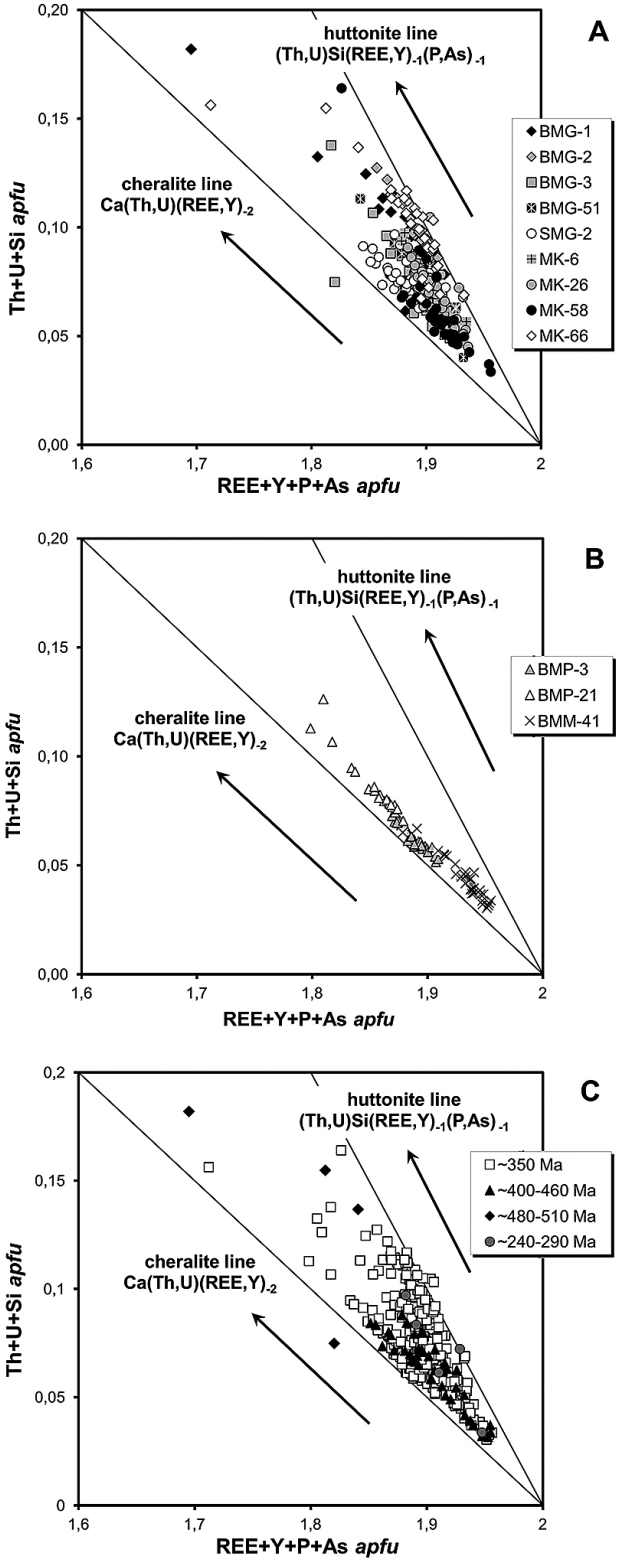

Fig. 5. Substitution Th+U+Si vs. REE+Y+P+As diagrams of monazite-(Ce) from the Bratislava Massif. A: granitic rocks, B: pegmatites and paragneiss, C: from different age populations.

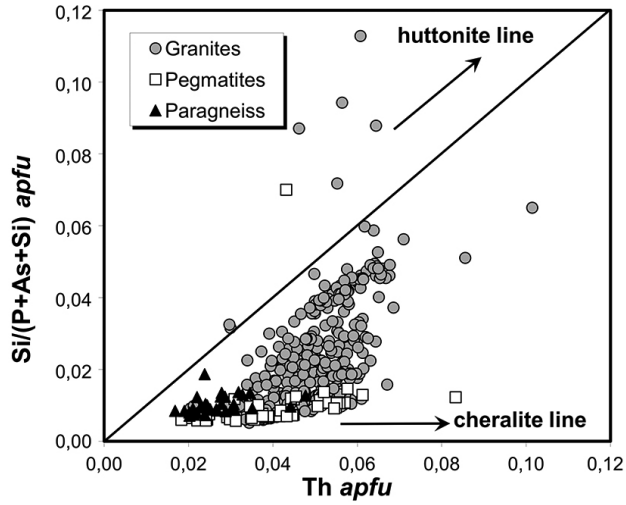

Fig. 6. Si/(P+As+Si) vs. Th diagram of monazite-(Ce) from studied granites, pegmatites and paragneiss of the Bratislava Massif. The positions of the analyses above huttonite line are probably due to microinclusions of quartz in monazite.

most stable REE-rich phase of peraluminous (often garnet-bearing) and low-Ca, collision-related granitic suites, commonly with S-type or highly evolved I-type affiliation (e.g., Broska & Uher, 1991; Bea, 1996; Förster, 1998; Kelts et al., 2008; Petrík & Konečný, 2009).

Monazite from the BGM granitic rocks are locally enriched in Th (≤9 wt. % ThO_2), whereas monazite from the pegmatites (especially from Bratislava, Rössler quarry) show uranium-rich zones (≤4 wt. % UO_2). Both huttonite $ThSiREE_{-1}P_{-1}$ and cheralite $CaThREE_{-2}$ substitutions control the entry of Th and U into the monazite structure. Both the huttonite and cheralite substitutions are observed in monazite of the BGM granitic rocks, whereas cheralite substitution is dominant in both pegmatite samples and the paragneiss (Fig. 5). The increasing of Si and huttonite ($ThSiO_4$) molecule in monazite from granite-pegmatite systems is believed to be proportionally to higher temperatures (Broska et al., 2000). On the other hand, monazite formed at lower-temperature, more evolved and volatile-rich granites and granitic pegmatites commonly shows high Th and U contents due to enrichment in cheralite ($Ca_{0.5}Th_{0.5}PO_4$) and $Ca_{0.5}U_{0.5}PO_4$ molecules (Gramaccioli & Segalstad, 1978; Bea, 1996; Förster, 1998; Pérez-Soba et al., 2014; Uher et al., 2014). However, some monazite-huttonite s.s. from granitic pegmatites reveal anomalously high Si contents (up to 13.5 wt. % SiO_2; Kucha, 1980; Popova & Churin, 2010). Therefore, the behaviour of Th and U in natural monazites is complex and not unambiguous (e.g., Catlos, 2013).

5.2. Age of Bratislava Massif

The age of the BGM based on field geological relationships has been ambiguous in historical context; Richarz (1908) assumed the Alpine, post-Liassic age on the basis of wrong observations of the granite-related contact metamorphic overprint on Mesozoic (Liassic) limestones in the Hainburg castle hill. However, other authors suggested the Hercynian (Variscan) age (e.g., Koutek

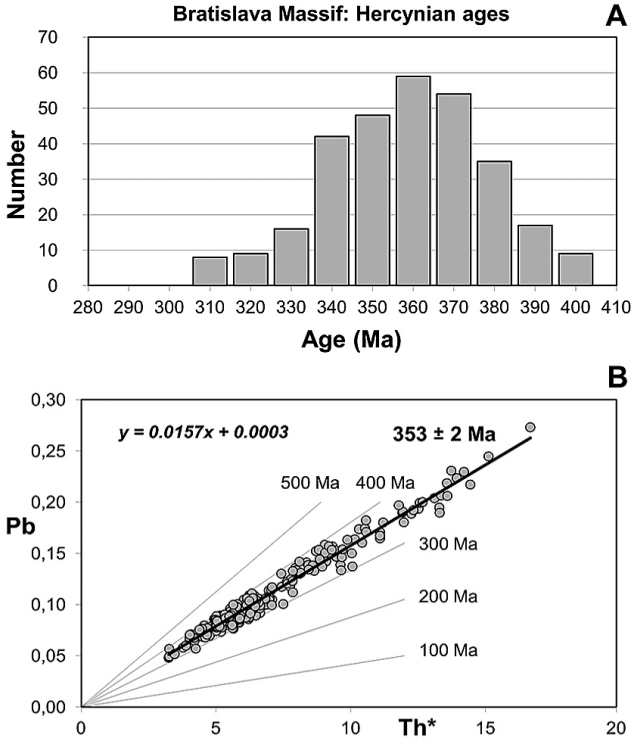

Fig. 7. Histogram (A) and isochron diagram (B) of Hercynian monazite-(Ce) ages from the studied granitic rocks and pegmatites of the Bratislava Massif. Pb values are in wt. %, Th* = Th + 3.15*U wt. %.

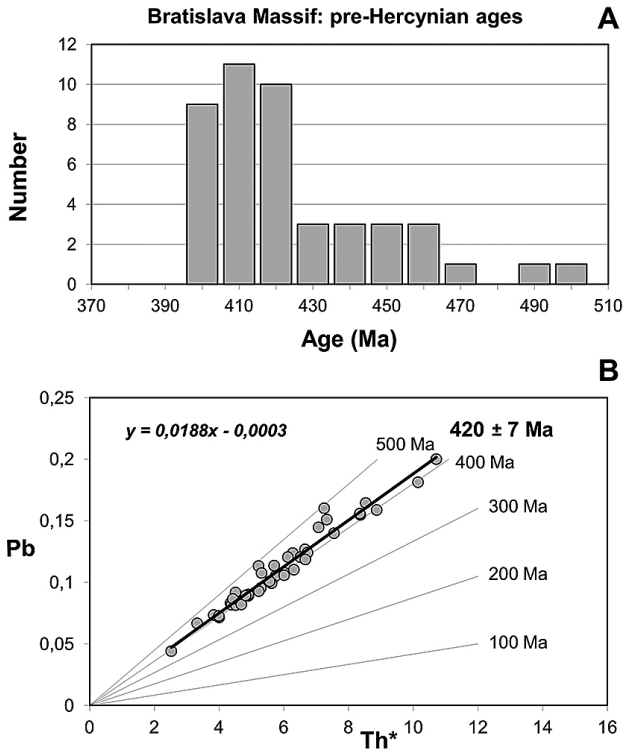

Fig. 8. Histogram (A) and isochron diagram (B) of pre-Hercynian monazite-(Ce) ages from the studied granitic rocks of the Bratislava Massif. Pb values are in wt. %, Th* = Th + 3.15*U wt. %.

& Zoubek, 1936), confirmed by findings of analogous granitic rocks as pebbles in the Permian (?) to Lower Triassic arkoses to quartzites (Cambel & Valach, 1956).

The first K-Ar isotopic geochronological data of K-feldspar and micas from BGM also indicated mainly the Upper Paleozoic, Hercynian ages (Kantor, 1959, 1961; Bagdasaryan et al., 1977). Later, Rb-Sr dating confirmed the Hercynian age of BGM with a 347 ± 4 Ma whole-rock isochron (Bagdasaryan et al., 1982), whereas biotite-whole rock and especially biotite-muscovite Rb-Sr isochrons indicated generally younger ages (Cambel et al., 1979, 1990; Bagdasaryan et al., 1982). Preliminary results of Th-U-Pb electron-microprobe monazite dating of BGM revealed the Lower Carboniferous, Hercynian age (355 ± 18 Ma, Finger et al., 2003). Recently, the Hercynian, 355 ± 5 Ma age of BGM has been confirmed also by zircon U-Th-Pb SHRIMP dating (Kohút et al., 2009).

Consequently, there is no more doubt of the Hercynian age of magmatic solidification. However, the K-Ar ages from BGM show a large variation (379 to 233 Ma) due to released internal fluids during rapid cooling and/or the partial Alpine overprint. Similarly, whole-rock – mineral (biotite, muscovite) Rb-Sr isochrons (279 to 159 Ma) indicate post-crystallisation opening of system or alteration, although whole-rock isochron gave a rather reasonable age 347 ± 4 Ma from the magmatic crystallisation point of view (Bagdasaryan et al., 1982). Our robust result (353 ± 2 Ma) based on 290 spot dating measurements is thus in excellent accordance with published monazite age from this massif 355 ± 18 Ma (Finger et al., 2003) done from limited spot measurements (n = 10), as well as SHRIMP zircon dating (355 ± 5 Ma, Kohút et al., 2009).

The age of the inherited monazite population, locally preserved in monazite crystals from some granitic rocks of BGM show a relatively wide interval of ~505 to 400 Ma, with an average calculated isochron age of 420 ± 7 Ma (Table 4, Fig. 8B), which corresponds to the Silurian–Devonian boundary (International chronostratigraphic chart, version 2014/02). These pre-Hercynian ages probably indicate a presence of older clastic monazite grains and/or low-temperature authigenic to metamorphic monazite inherited from pelitic to psammitic metasedimentary rocks, a main protolith of the S-type granites of the BGM. Moreover, the main population of the older, pre-intrusion monazite ages (420–400 Ma) roughly corresponds to age of the first, regional metamorphic overprint of the metapelites to metapsammites around the BGM under the greenschist facies, as revealed by Rb-Sr isochron dating (387 ± 38 Ma – Bagdasaryan et al., 1983; 380 ± 20 Ma – Cambel et al., 1990).

5.3. Meso-Hercynian granitic plutonism of the Western Carpathians and geodynamic implications

The Lower Carboniferous (Mississippian) age of ~ 350 ± 10 Ma represents the dominant magmatic event for the origin of S- and I-type granitic rocks in the West-Carpathian Hercynian Belt (WCHB). The dominancy of the ~ 350 ± 10 Ma magmatism in the WCHB is documented by numerous U-Pb zircon ages from the Tatric Unit, e.g., the Malá Fatra Mountains: 353 ± 11 Ma

(Scherbak et al., 1990), the Veľká Fatra Mts.: 356 ± 25 Ma (Kohút et al., 1997), the Strážovské Vrchy Mts.: 356 ± 9 Ma (Kráľ et al., 1997), the Tatry Mts.: 347 ± 14 Ma to 357 ± 7 Ma (Poller et al., 2000, 2001) and 350 ± 5 Ma (Burda et al., 2013), the Nízke Tatry Mts.: 353–356 ± 3 Ma (Broska et al., 2013); as well as from the Veporic Unit: the Sinec type: 350 ± 5 Ma (Bibikova et al., 1988), the Kráľova Hoľa type: 345 ± 11 Ma (Gaab et al., 2005), and the Sihla type: 357 ± 2 Ma (Broska et al., 2013). Isochrone Rb-Sr and electron-microprobe Th-U-Pb monazite dating of the West-Carpathian Hercynian granitic suites yields commonly analogous ages (e.g., Bagdasaryan et al., 1982, 1990; Cambel et al., 1990; Finger et al., 2003, and references therein). Moreover, the Hercynian metamorphic overprint of older, probably the Ordovician orthogneisses in the Nízke Tatry and Vepor Mts., gave an analogous, 340–350 Ma age interval by monazite chemical dating (Petrík et al., 2006; Ondrejka et al., 2012). In-situ SHRIMP zircon U-Th-Pb dating from I-type granitic suites also revealed an age interval of 347 ± 4 Ma for the Modra Granitic Massif (Kohút et al., 2009). Moreover, slightly older, the Devonian to Mississipian ages (~360 to 370 Ma) were determinated for the anatectic migmatites of the Western Tatra Mts.: 359 ± 1 to 365 ± 2 Ma (Burda, 2007) and 368 ± 8 Ma (Burda et al., 2011) and granites of the Tribeč Mts.: 358 to 367 ± 3 Ma (Broska et al., 2013).

The geodynamic evolution of the WCHB is generally comparable to the Variscan (Hercynian) orogenic belt of western and central Europe, mainly in the Massif Central and the Bohemian Massif, where dominant I-type granitic rocks emplaced during ~360 to 350 Ma period, e.g., in the Central Bohemian Granitic Belt (Finger et al., 2009; Janoušek et al., 2004, 2010). A similar evolution was suggested for crystalline basement of the Alpine-Carpathian realm (e.g., Franke, 1992; von Raumer & Neubauer, 1993; Stampfli, 1996; Plašienka et al., 1997; Petrík & Kohút, 1997; Broska et al., 2013). Generally, the collision of two major continental plates: Gondwana and Baltica (Laurasia), caused the closure of Paleotethys ocean, subsequent collision of minor continental fragments evolved from the disruption of the northern margin of Gondwana (including the Galatian superterrane, where probably an original area of WCHB was situated), and initiated partial melting, intrusion and emplacement of the meso-Hercynian granitic suites in the Western Carpathians (Broska et al., 2013).

Acknowledgements: This work was supported by the Slovak Research and Development Agency under the contracts No. APVV-0557-06, APVV-0549-07, APVV-0081-10 and VEGA Agency No. 1/0257/13. The early version of manuscript benefited from constructive comments by F. Corfu and Š. Méres.

References

Bagdasaryan G.P., Cambel B., Veselský J. & Gukasyan R.Ch., 1977: Kalium-argon age determinations of the West-Carpathian crystalline complexes and preliminary interpretation of the results. *Geologický Zborník Geologica Carpathica,* 28, 2, 219–242 (in Russian).

Bagdasaryan G.P., Gukasyan R.Ch., Cambel B. & Veselský J., 1982: The age of Malé Karpaty Mts. granitoid rocks determined by Rb-Sr isochrone method. *Geologický Zborník Geologica Carpathica,* 33, 2, 131–140.

Bagdasaryan G.P., Gukasyan R.Ch., Cambel B. & Veselský J., 1983: The results of Rb-Sr dating of the Malé Karpaty Mts. crystalline complex metamorphic rocks. *Geologický Zborník Geologica Carpathica,* 34, 4, 387–397 (in Russian).

Bagdasaryan G.P., Gukasyan R.Kh., Cambel B. & Broska, I., 1990: Rb-Sr isochrone dating of granitoids from Tríbeč Mts. *Geologický Zborník Geologica Carpathica*, 41, 4, 437–442.

Bea F., 1996: Resistence of REE, Y, Th and U in granites and crustal protoliths; implications for the chemistry of crustal melts. *Journal of Petrology*, 37, 3, 521–552.

Bibikova E.V., Cambel B., Korikovsky S.P., Broska I., Gracheva T.V., Makarov V.A. & Arakeliants M.M., 1988: U-Pb and K-Ar isotopic dating of Sinec (Rimavica) granites (Kohút zone of Veporides). *Geologický Zborník Geologica Carpathica,* 39, 2, 147–157.

Bingen B., Demaiffe D. & Hertogen J., 1996: Redistribution of rare earth elements, thorium, and uranium over accessory minerals in the course of amphibolite to granulite facies metamorphism: The role of apatite and monazite in orthogneisses from southwestern Norway. *Geochimica et Cosmochimica Acta*, 60, 8, 1341–1354.

Broska I. & Siman P., 1998: The breakdown of monazite in the West-Carpathian Veporic orthogneisses and Tatric granites. *Geologica Carpathica*, 49, 3, 161–167.

Broska I. & Uher P., 1991: Regional typology of zircon and its relationship to allanite/monazite antagonism (on an example of Hercynian granitoids of Western Carpathians). *Geologica Carpathica*, 42, 5, 271–277.

Broska I. & Uher P., 2001: Whole-rock chemistry and genetic typology of the West-Carpathian Variscan Granites. *Geologica Carpathica*, 52, 2, 79–90.

Broska I., Petrík I. & Williams C.T., 2000: Co-existing monazite and allanite in peraluminous granitoids of the Tribeč Mountains, Western Carpathians. *American Mineralogist*, 85, 1, 22–32.

Broska I., Petrík I., Be´eri-Shlevin Y., Majka J. & Bezák V., 2013: Devonian/Mississippian I-type granitoids in the Western Carpathians: A subduction-related hybrid magmatism. *Lithos*, 162–163, 27–36.

Burda J., 2007: U-Pb zircon and monazite dating of partial melting in migmatitic metapelites from Western Tatra Mts. *Granitoids in Poland*, AM Monograph No. 1, 333–340.

Burda J., Gawęda A. & Klötzli U., 2011: Magma hybridization in the Western Tatra Mts. granitoid intrusions (S-Poland, Western Carpathians). *Mineralogy and Petrology*, 103, 1–4, 19–36.

Burda J., Gawęda A. & Klötzli U., 2011: Geochronology and petrogenesis of granitoid rocks from the Goryczkowa Unit, Tatra Mountains (Central Western Carpathians). *Geologica Carpathica*, 64, 6, 419–435.

Cambel B. & Čorná O., 1974: Stratigraphy of crystalline basement of the Malé Karpaty massif in the light of the palynological investigations. *Geologický Zborník Geologica Carpathica*, 25, 2, 231–241 (in Russian).

Cambel B. & Planderová E., 1985: Biostratigraphic evaluation of metasediments in the Malé Karpaty Mts. region. *Geologický Zborník Geologica Carpathica*, 36, 6, 683–700.

Cambel B. & Valach J., 1956: Granitoid rocks of the Malé Karpaty Mountains: geology, petrography and petrochemistry. *Geologické Práce, Zošit*, 42, 113–268 (in Slovak).

Cambel B. & Vilinovič V., 1987: Geochémia a petrológia granitoidných hornín Malých Karpát (Geochemistry and petrology of the granitoid rocks of the Malé Karpaty Mts.). *Veda*, Bratislava, 148 p. (in Slovak with English summary).

Cambel B., Bagdasaryan G.P., Veselský J. & Gukasyan R.C., 1979: New Rb-Sr and K-Ar age data of Slovak rocks and their interpretation possibilities. *Geologický Zborník Geologica Carpathica*, 30, 1, 45–60 (in Russian).

Cambel B., Dyda M. & Spišiak J., 1981: Thermodynamic measurements of origin of minerals in metamorphites in the area of crystalline of Malé Karpaty Mts. *Geologický Zborník Geologica Carpathica*, 32, 6, 745–768.

Cambel B., Kráľ J. & Burchart J., 1990: Izotopová geochronológia kryštalinika Západných Karpát s katalógom údajov (Isotope geochronology of the Western Carpathian crystalline complex with catalogue of data). *Veda*, Bratislava, 184 p. (in Slovak with English summary).

Catlos E.J., 2013: Generalizations about monazite: Implications for geochronologic studies. *American Mineralogist, 98, 5–6, 819–832.*

Cocherie A. & Albarede F., 2001: An improved U-Th-Pb age calculation for electron microprobe dating of monazite. *Geochimica et Cosmochimica Acta*, 65, 24, 4509–4522.

Čorná O., 1968: Sur la trouvaille de restes ďorganismes dans les roches graphitiques du cristallin des Petites Carpathes. *Geologický Zborník Geologica Carpathica*, 19, 2, 303–309.

Černý P. & Ercit T.S., 2005: The classification of granitic pegmatites revisited. *The Canadian Mineralogist*, 43, 6, 2005–2026.

Chudík P., Uher P., Gadas P., Škoda R. & Pršek J., 2011: Niobium-tantalum oxide minerals in the Jezuitské Lesy granitic pegmatite, Bratislava Massif, Slovakia: Ta to Nb and Fe to Mn evolutionary trends in a narrow Be,Cs-rich and Li,B-poor dike. *Mineralogy and Petrology*, 102, 1–4, 15–27.

Dávidová Š., 1970: Charakteristik der Pegmatite der Kleinen Karpaten. *Geologický Zborník Geologica Carpathica,* 21, 1, 115–137.

Dyda M., 1997: Disturbance of the Variscan metamorphic complex indicated by mineral reaction, P-T data and crystal size of garnets (Malé Karpaty Mts.). *In:* Grecula P., Hovorka D. & Putiš M., (Eds.): Geological evolution of the Western Carpathians. *Mineralia Slovaca Monograph*, Bratislava, 333–342.

Dyda M., 2000: Exhumation and cooling rates of the Variscan basement metamorphic complex inferred from petrological data (Malé Karpaty Mts.). *Slovak Geological Magazine*, 6, 2–3, 293–297.

Finger F. & Krenn E., 2007: Three metamorphic monazite generations in a high-pressure rock from the Bohemian Massif and the potentially important role of apatite in stimulating polyphase monazite growth along a PT loop. *Lithos,* 95, 1–2, 103–115.

Finger F., Broska I., Roberts M.P. & Schermaier A., 1998: Replacement of primary monazite by apatite-allanite-epidote coronas in an amphibolite facies granite gneiss from the eastern Alps. *American Mineralogist*, 83, 3–4, 248–258.

Finger F., Broska I., Haunschmid B., Hraško Ľ., Kohút M., Krenn E., Petrík I., Riegler G. & Uher P., 2003: Electron-microprobe dating of monazites from Western Carpathian basement granitoids: plutonic evidence for an important Permian rifting event subsequent to Variscan crustal anatexis. *International Journal of Earth Sciences*, 92, 1, 86–98.

Finger F., Gerdes A., René M. & Riegler G., 2009: The Saxo-Danubian Granite Belt: magmatic response to postcollisional delamination of mantle lithosphere below the southwestern sector of the Bohemian Massif (Variscan orogen). *Geologica Carpathica*, 60, 3, 205–212.

Förster H.-J., 1998: The chemical composition of REE-Y-Th-U-rich accessory minerals in peraluminous granites of the Erzgebirge-Fichtelgebirge region, Germany, Part I: The monazite-(Ce)-brabantite solid solution series. *American Mineralogist*, 83, 3–4, 259–272.

Franke W., 1992: Phanerozoic structures and events in Central Europe. *In:* Blundel D., Freeman R. & Mueller S. (Eds.): A continent revealed. The European geotraverse. *Cambridge University Press*, 164–180.

Gaab A.S., Poller U., Janák M., Kohút M. & Todt W., 2005: Zircon U-Pb geochronology and isotopic characterization for the pre-Mesozoic basement of the Northern Veporic Unit (Central Western Carpathians, Slovakia). *Schweizerische Mineralogische und Petrographische Mitteilungen*, 85, 1, 69–88.

Gramaccioli C.M. & Segalstad T.V., 1978: A uranium- and thorium-rich monazite from a south-Alpine pegmatite at Piona, Italy. *American Mineralogist*, 63, 7–8, 757–761.

Ivan P., Méres Š., Putiš M. & Kohút M., 2001: Early Paleozoic metabasalts and metasedimentary rocks from the Malé Karpaty Mts. (Western Carpathians): Evidence for rift basin and ancient oceanic crust. *Geologica Carpathica*, 52, 2, 67–78.

Ivan P. & Méres Š., 2006: Litostratigrafické členenie a pôvod staropaleozoickej časti kryštalinika Malých Karpát – nový pohľad na základe výsledkov geochemického výskumu. *Mineralia Slovaca*, 38, 2, 165–186.

Janoušek V., Braithwaite C.J.R., Bowes D.R. & Gerdes A., 2004: Magma-mixing in the genesis of Hercynian calc-alkaline granitoids: an integrated petrographic and geochemical study of the Sázava intrusion, Central Bohemian Pluton, Czech Republic. *Lithos*, 78, 1–2, 67–99.

Janoušek V., Wiegand B.A. & Žák J., 2010: Dating the onset of Variscan crustal exhumation in the core of the Bohemian Massif: new U–Pb single zircon ages from the high-K calc-alkaline granodiorites of the Blatná suite, Central Bohemian Plutonic complex. *Journal of the Geological Society*, 167, 2, 347–360.

Johan Z. & Johan V., 2005: Accessory minerals of the Cínovec (Zinnwald) granite cupola, Czech Republic: indicators of petrogenetic evolution. *Mineralogy and Petrology*, 83, 1–2, 113–150.

Kantor J., 1959: Contribution to age knowledge of some granites and related mineral deposits of the Western Carpathians. *Acta Geologica et Geographica Universitatis Comeniana, Geologica,* 2, 63–73.

Kantor J., 1961: Beitrag zur Geochronologie der Magmatite und Metamorphite des westkarpatischen Kristallins. *Geologické Práce, Zošit*, 60, 303–317.

Kelts A.B., Ren M. & Anthony E.Y., 2008: Monazite occurrence, chemistry, and chronology in the granitoid rocks of the Lachlan Fold Belt, Australia: An electron microprobe study. *American Mineralogist*, 93, 2–3, 373–383.

Kohút M., Todt W., Janák M. & Poller U., 1997: Thermochronometry of the Variscan basement exhumation in the Veľká Fatra Mts. (Western Carpathians, Slovakia). *Terra Abstracts*, 9, EUG 9, Strasbourg, 494.

Kohút M., Uher P., Putiš M., Ondrejka M., Sergeev S., Larionov A. & Paderin I., 2009: SHRIMP U-Th-Pb zircon dating of the granitoid massifs in the Malé Karpaty Mountains (Western Carpathians): evidence of Meso-Hercynian successive S- to I-type granitic magmatism. *Geologica Carpathica*, 60, 5, 345–350.

Konečný P., Siman P., Holický I., Janák M. & Kollárová V., 2004:Merodika datovania monazitu pomocou elektrónového mikroanalyzárora (Metodics of monazite dating using an electron microprobe). *Mineralia Slovaca*, 36, 3–4, 225–235.

Korikovsky S.P., Cambel B., Miklós J. & Janák M., 1984: Metamorphism of the Malé Karpaty crystalline complex: stages, zonality, relationship to granitic rocks. *Geologický Zborník Geologica Carpathica*, 35, 4, 437–462 (in Russian).

Koutek J. & Zoubek V., 1936: Vysvětlivky ke geologické mapě v měřítku 1:75 000. List Bratislava 4758. *Knihovna Státního Geologického Ústavu Československé Republiky*, 18, 150 p.

Kráľ J., Hess C., Kober B. & Lippolt H.J., 1997: $^{207}Pb/^{206}Pb$ and $^{40}Ar/^{39}Ar$ age data from plutonic rocks of the Strážovské vrchy Mts. basement, Western Carpathians. *In:* Grecula P., Hovorka D. & Putiš M. (Eds): Geological evolution of the Western Carpathians. *Mineralia Slovaca. Monograph*, Bratislava, 253–260.

Krenn E. & Finger F., 2007: Formation of monazite and rhabdophane at the expense of allanite during Alpine low temperature retrogression of metapelitic basement rocks from Crete, Greece: Microprobe data and geochemical implications. *Lithos*, 95, 1–2, 130–147.

Krist E., Korikovskij S.P., Putiš M., Janák M. & Faryad S.W., 1992: Geology and petrology of metamorphic rocks of the Western Carpathian crystalline complex. *Comenius University Press,* Bratislava, 324 p.

Kucha H., 1980: Continuity in the monazite-huttonite series. *Mineralogical Magazine*, 43, 332, 1031–1034.

Méres Š., 2005: Major, trace element and REE geochemistry of metamorphosed sedimentary rocks from the Malé Karpaty Mts. (Western Carpathians, Slovak Republic): Implications for sedimentary and metamorphic processes. *Slovak Geological Magazine*, 11, 2–3, 107–122.

Mišík M., 1955: Akcesorické minerály malokarpatských žulových masívov. *Geologický Sborník Slovenskej Akadémie Vied*, 6, 3–4, 161–174.

Montel, J.M., 1993: A model for monazite/melt equilibrium and application to the generation of granitic magmas. *Chemical Geology*, 110, 1–3, 127–146.

Montel J.-M., Foret S., Vescambre M., Nicollet C. & Provost A., 1996: Electron microprobe dating of monazite. *Chemical Geology*, 131, 1–4, 37–53.

Ondrejka M., Uher P., Pršek J. & Ozdín D., 2007: Arsenian monazite-(Ce) and xenotime-(Y), REE arsenates and carbonates from the Tisovec-Rejkovo rhyolite, Western Carpathians, Slovakia: Composition and substitutionsin the $(REE,Y)XO_4$ system (X = P, As, Si, Nb, S). *Lithos*, 95, 1–2, 116–129.

Ondrejka M., Uher P., Putiš M., Broska I., Bačík P., Konečný P. & Schmiedt I., 2012: Two-stage breakdown of monazite by post-magmatic and metamorphic fluids: An example from the Veporic orthogneiss, Western Carpathians, Slovakia. *Lithos*, 142–143, 245–255.

Pérez-Soba C., Villaseca C., Orejama D. & Jeffries T., 2014: Uranium-rich accessory minerals in the peraluminous and perphosphorous Belvís de Monroy pluton (Iberian Variscan belt). *Contributions to Mineralogy and Petrology*, 167, 5, 1008, 1–25.

Petrík I. & Kohút M., 1997: The evolution of granitoid magmatism during the Hercynian Orogen in the Western Carpathians. *In:* Grecula P., Hovorka D. & Putiš M. (Eds): Geological evolution of the Western Carpathians. *Mineralia Slovaca, Monograph*, Bratislava, 235–252.

Petrík I. & Konečný P., 2009: Metasomatic replacement of inherited metamorphic monazite in a biotite-garnet granite from the Nízke Tatry Mountains, Western Carpathians, Slovakia: Chemical dating and evidence for disequilibrium melting. *American Mineralogist*, 94, 7, 957–974.

Petrík I., Kohút M. & Broska I. (Eds.) 2001: Granitic plutonism of the Western Carpathians. Guide book to Eurogranites 2001. *Veda*, Bratislava, 116 p.

Petrík I., Konečný P., Kováčik M. & Holický I., 2006: Electron microprobe dating of monazite from the Nízke Tatry Mountains orthogneisses (Western Carpathians, Slovakia). *Geologica Carpathica*, 57, 4, 227–242.

Plašienka D., Grecula P., Putiš M., Kováč M. & Hovorka D., 1997: Evolution and structure of the Western Carpathians: an overview. *In:* Grecula P., Hovorka D. & Putiš M. (Eds.): Geological evolution of the Western Carpathians. *Mineralia Slovaca, Monograph*, Bratislava, 1–24.

Poller U., Janák M., Kohút M. & Todt W., 2000: Early Variscan Magmatism in the Western Carpathians: U-Pb zircon data from granitoids and orthogneisses of the Tatra Mts. (Slovakia). *International Journal of Earth Sciences*, 89, 2, 336–349.

Poller U., Todt W., Kohút M. & Janák M., 2001: Nd, Sr, Pb isotope study of the Western Carpathians: implications for Paleozoic evolution. *Schweizeriche Mineralogische und Petrographische Mitteilengen*, 81, 2, 159–174.

Popova V.I. & Churin E.I., 2010: Zoning and sectoriality of monazite-(Ce) from granite pegmatites of the Central and South Urals. *Geology of Ore Deposits*, 52, 7, 646–655.

Putiš M., Hrdlička M. & Uher P., 2004: Litológia a gtanitoidný magmatizmus staršiehio paleozoika Malých Karpát. *Mineralia Slovaca*, 36, 3–4, 183–194.

Richarz P.S., 1908: Der südliche Teil der Kleinen Karpathen und die Hainburger Berge. *Jahrbuch der Kaiserlich-Königlichen Geologischen Reichsanstalt*, 58, 1, 1–48.

Scherbak N.P., Cambel. B., Bartnicky E.N. & Stepanyuk L.M., 1990: U-Pb age of granitoid rock from Dubná skala – Malá Fatra Mts. *Geologický Zborník Geologica Carpathica*, 41, 4, 407–414.

Scherrer N.C., Engi M., Gnos E., Jakob V. & Liechti A., 2000: Monazite analysis; from sample preparation to microprobe age dating and REE quantification. *Schweizeriche Mineralogische und Petrographische Mitteilengen*, 80, 1, 93–105.

Stampfli G.M., 1996: The Intra-Alpine terrain: A Paleothethyan remnant in the Alpine Variscides. *Eclogae Geologicae Helvetiae*, 89, 1, 13–42.

Suzuki K., Adachi M. & Tanaka T., 1991: Middle Precambrian provenance of Jurassic sandstone in the MinoTerrane, central Japan: Th-U-total Pb evidence from an electron microprobe monazite study. *Sedimentary Geology*, 75, 1–2, 141–147.

Uher P., 1994: The Variscan West-Carpathian granitic pegmatites: mineralogy, petrogenesis and relationship to pegmatite populations in the Eastern Alps and Romanian Carpathians. *Geologica Carpathica*, 45, 5, 313–318.

Uher P. & Broska I. 1995: Pegmatites in two suites of Variscan orogenic rocks (Western Carpathians, Slovakia). *Mineralogy and Petrology*, 55, 1–3, 27–36.

Uher P., Chudík P., Bačík P., Vaculovič T. & Galiová M., 2010: Beryl composition and evolution trends: an example from granitic pegmatites of the beryl-columbite subtype, Western Carpathians, Slovakia. *Journal of Geosciences*, 55, 1, 69–80.

Uher P., Janák M., Konečný P. & Vrabec M., 2014: Rare-element granitic pegmatite of Miocene age emplaced in UHP rocks from Visole, Pohorje Mountains (Eastern Alps, Slovenia): accessory minerals, monazite and uraninite chemical dating. *Geologica Carpathica*, 65, 2, 131–146.

Veselský J., 1972: Akzessorische Minerale granitoider Gesteine der Kleinen Karpaten. *Geologický Zborník Geologica Carpathica*, 23, 1, 115–131.

Veselský J. & Gbelský J., 1978: Výsledky štúdia akcesorických minerálov granitoidov a pegmatitov Malých Karpát. *Acta Geologica et Geographica Universitatis Comeniana, Geologica,* 33, 91–112.

Vojtko P., Janák M. & Broska I., 2011[a]: Thermodynamic modeling of P-T conditions in staurolite-bearing metapelites of the Malé Karpaty Mts. *In:* Ondrejka M. & Šarinová K. (Eds.): Termodynamické modelovanie petrologických procesov. *Petros 2011*. Univerzita Komenského v Bratislave, Bratislava, p. 60.

Vojtko P., Broska I. & Ševčík R., 2011[b]: Identifikácia rotácie staurolitu z metapelitov počítačovým mikrotomografom (Záhorská Bystrica, Malé Karpaty). (Identification of the rotation of staurolite by computed microtomography (Záhorská Bystrica, Malé Karpaty)). *Mineralia Slovaca*, 43, 3, 305–312 (in Slovak).

von Raumer J.F. & Neubauer F., 1993: Late Proterozoic and Paleozoic evolution of the Alpine basement - an overview. *In:* von Raumer J.F. & Neubauer F., (Eds.): Pre-Mesozoic Geology of Alps. *Springer*, Berlin, New York, 625–639.

Williams M.L., Jercinovic M.J., Goncalves P. & Mahan K., 2006: Format and philosophy for collecting, compiling, and reporting microprobe monazite ages. *Chemical Geology*, 225, 1–15.

Zhu X.K. & O`Nions R.K., 1999: Monazite chemical composition: some implications for monazite geochronology. *Contributions to Mineralogy and Petrology*, 137, 4, 351–363.

Appendix: Sample location

For U-Th-Pb electron-microprobe monazite dating the following samples were measured (Fig. 1):

BMG-1: medium-grained, equigranular biotite granodiorite. Bratislava, Devín, large active quarry, 3200 m/150° from Devínska Kobyla (altitude point 514.1 m asl.).

BMG-2: medium-grained, slightly porphyric biotite monzogranite. Bratislava, Devín, large active quarry, 3200 m/150° from Devínska Kobyla (altitude point 514.1 m asl.).

BMG-3: fine-grained, equigranular muscovite-biotite granodiorite. Bratislava, abandoned Rössler quarry, 1950 m/90° from Kamzík (altitude point 439.4 m asl.).

BMP-3: granitic pegmatite dike in BMG-3 granodiorite, coarse-grained K-feldspar–albite–quartz-biotite-muscovite zone. Bratislava, abandoned Rössler quarry, 1950 m/90° from Kamzík (altitude point 439.4 m asl.).

BMP-21: granitic pegmatite dike in granitic rocks. Bratislava, Dúbravka, natural outcrop, 450 m/75° from Švábsky vrch (altitude point 359.8 m asl.).

BMG-51: medium-grained, porphyric muscovite-biotite granodiorite. Bratislava, Devín, natural outcrop ca. 500 m SE of Devín village, 2500 m/180° from Devínska Kobyla (altitude point 514.1 m asl.).

SMG-2: medium-grained, equigranular biotite granodiorite. Pezinok, old dumps of the Staré Mesto gold deposit, 1300 m/105° from Konské Hlavy (altitude point 648.8 m asl.).

MK-6: fine-grained, equigranular muscovite-biotite granodiorite. Bratislava, Rača, small natural outcrop, 150 m/260° from Veľký Javorník (altitude point 593.7 m asl.).

MK-26: fine- to medium-grained, equigranular muscovite-biotite monzogranite. Borinka, Popálené, small natural outcrop, 1150 m/295° from Malý Javorník (altitude point 583.7 m asl.).

MK-58: medium-grained, slightly porphyric, muscovite-biotite monzogranite. Svätý Jur, Človečia Hlava, small natural outcrop, 1450 m/65° from Veľký Javorník (altitude point 593.7 m asl.).

MK-66: medium-grained, slightly porphyric biotite granodiorite. Bratislava, Devín, large active quarry, 3200 m/150° from Devínska Kobyla (altitude point 514.1 m asl.).

BMM-41: Biotite paragneiss with chlorite, garnet and staurolite. Limbach, Slnečné Valley, natural outcrop, 900 m/210° from Žilová Hill (altitude point 447.5 m asl.).